Modelling Silicate – Nitrate - Ammonium co-limitation of algal growth and the importance of bacterial remineralisation based on an experimental Arctic coastal spring bloom culture study

Tobias R. Vonnahme[1], Martial Leroy[2], Silke Thoms[3], Dick van Oevelen[4], H. Rodger Harvey[5], Svein Kristiansen[1], Rolf Gradinger[1], Ulrike Dietrich[1], Christoph Voelker[3]

[1] Department of Arctic and Marine Biology, UiT – The Arctic University of Norway, Tromsø, Norway
[2] Université Grenoble Alpes, Grenoble, France
[3] Alfred-Wegener Institute for Polar and Marine Research, Bremerhaven, Germany
[4] Department of Estuarine and Delta Systems, NIOZ Royal Netherlands Institute for Sea Research, and Utrecht University, Texel, Yerseke, Netherlands
[5] Department of Ocean and Earth Sciences, Old Dominion University, Norfolk, USA

Correspondence to: Tobias R. Vonnahme (Tobias.Vonnahme@uit.no) and Christoph Voelker (christoph.voelker@awi.de)

Abstract. Arctic coastal ecosystems are rapidly changing due to climate warming. This makes modelling their productivity crucially important to better understand future changes. System primary production in these systems is highest during the pronounced spring bloom, typically dominated by diatoms. Eventually the spring blooms terminate due to silicon or nitrogen limitation. Bacteria can play an important role for extending bloom duration and total CO_2 fixation through ammonium regeneration. Current ecosystem models often simplify the effects of nutrient co-limitations on algal physiology and cellular ratios and simplify nutrient regeneration. These simplifications may lead to underestimations of primary production. Detailed biochemistry- and cell-based models can represent these dynamics but are difficult to tune in the environment. We performed a cultivation experiment that showed typical spring bloom dynamics, such as extended algal growth via bacterial ammonium remineralisation, reduced algal growth and inhibited chlorophyll synthesis under silicate limitation, and gradually reduced nitrogen assimilation and chlorophyll synthesis under nitrogen limitation. We developed a simplified dynamic model to represent these processes. Overall, model complexity (number of parameters) is comparable to the phytoplankton growth and nutrient biogeochemistry formulations in common ecosystem models used in the Arctic while improving the representation of nutrient co-limitation related processes. Such model enhancements that now incorporate increased nutrient inputs and higher mineralization rates in a warmer climate will improve future predictions in this vulnerable system.

1 Introduction

Marine phytoplankton are responsible for half of the CO_2 fixation on Earth (Field et al., 1998; Westberry et al., 2008). In high latitude oceans, diatoms are an important group contributing 20-40% of the global CO_2 fixation (Nelson et al., 1995; Uitz et al., 2010). Marine primary production can be bottom-up limited by light and/or nutrients like nitrogen (N), phosphorous (P), silicon (Si), and iron (Fe). Their availability is affected by pronounced geographical and seasonal variations (Eilertsen et al., 1989; Loebl et al., 2009; Iversen and Seuthe, 2011; Moore et al., 2013). Arctic coasts are one of the fastest changing systems due to climate change. Thus, modelling their dynamics is difficult but crucial for predictions of primary production with climate change (e.g. Slagstad et al., 2015; Fritz et al., 2017; Lannuzel et al., 2020). In Arctic coastal ecosystems, primary production is typically highest in spring. In spring, previous winter mixing supplied fresh nutrients and a stratified surface layer with sufficient light is facilitated by increasing temperatures and potentially sea ice melt (Sverdrup, 1953; Eilertsen et al., 1989; Eilertsen and Frantzen, 2007; Iversen and Seuthe, 2011). With increasing temperatures and runoff, stratification in coastal Arctic systems is expected to increase (Tremblay and Gagnon, 2009). This will lead to decreased mixing and nutrient upwelling in autumn and winter and an earlier stratified surface layer in spring, which may lead to an earlier spring bloom (Tremblay and Gagnon, 2009). However, at the same time, brownification and increased sediment resuspension is already leading to light inhibition in spring, which may lead to a delayed spring bloom (Opdal et al., 2019). The spring bloom typically consists of chain-forming diatoms and is terminated by Si or N limitation (Eilertsen et al., 1989; Iversen and Seuthe, 2011). Zooplankton grazing is typically of low importance for terminating blooms (e.g. Saiz et al., 2013), while inorganic nutrients are considered to drive bloom termination (Krause et al. 2019, Mills et al. 2018). Heterotrophic bacteria remineralisation of organic matter may supply additional N and Si (Legendre and Rassoulzadegan, 1995; Bidle and Azam, 1999; Johnson et al., 2007). N regeneration has been described as a mostly bacteria-related process (Legendre and Rassoulzadegan, 1995), while Si dissolution is mainly controlled by abiotic dissolution of silica (Bidle and Azam, 1999). Zooplankton may also release some ammonium and urea after feeding on phytoplankton, but we suggest that this process is likely far less important than bacterial regeneration (e.g. Saiz et al., 2013). Previously measured ammonium excretion of Arctic mesozooplankton is typically low compared to bacterial remineralization (Conover and Gustavson, 1999), with the exception for one study in summer in a more open ocean setting (Alcaraz et al., 2010). In some Arctic systems urea, excreted by zooplankton may be an important N source for regenerated algae production (Conover and Gustavson, 1999). A warmer climate will increase both bacteria-related remineralisation rates (Legendre and Rassoulzadegan, 1995; Lannuzel et al., 2020) and abiotic silica dissolution (Bidle and Azam, 1999). However, the magnitude is not well understood.

Phytoplankton blooms may be dominated by a single or a few algal species, often with a similar physiology during certain phases of the bloom (e.g. Eilertsen et al., 1989; Degerlund and Eilertsen, 2010; Iversen and Seuthe, 2011). Chain-forming centric diatoms share physiological needs and responses to nutrient limitations (e.g. Eilertsen et al., 1989; von Quillfeldt, 2005) and typically dominate these blooms. In some Arctic and sub-Arctic areas the Arctic phytoplankton species chosen for this model, *Chaetoceros socialis*, can be dominant during spring blooms (Rey and Skjoldal, 1987; Eilertsen et al., 1989; Booth et al., 2002; Ratkova and Wassmann, 2002; von Quillfeldt, 2005; Degerlund and Eilertsen, 2010). Such spring phytoplankton blooms are accompanied by heterotrophic bacterioplankton blooms also showing

typical succession patterns and distinct re-occurring taxa that dominate the community (Teeling et al., 2012; Teeling et al., 2016). The importance of bacterial nutrient recycling for regenerated production has been recognized in several ecosystem models (e.g. van der Meersche et al., 2004; Vichi et al., 2007; Weitz et al., 2015) and algae bioreactor models focussing on nutrient conversions (e.g. Zambrano et al., 2016). However, these models are typically highly simplified or omitted in more sophisticated dynamic multi-nutrient, quota based models (e.g. Flynn and Fasham, 1997b.; Wassmann et al., 2006; Ross and Geider, 2009). These latter models have been often developed and tuned based on cultivation experiments in which microbial remineralization reactions were assumed to be absent (e.g. Geider et al., 1998; Flynn, 2001) despite the fact that most algae cultures, likely including Geider et al., (1998) and Flynn (2001) are not axenic. Parameters estimated by fitting axenic models on non-axenic experiments may be misleading, mostly by an inflated efficiency of DIN uptake. Additional positive effects of bacteria include vitamin synthesis (Amin et al., 2012), trace metal chelation (Amin et al., 2012), the scavenging of oxidative stressors (Hünken et al., 2008), and exchange of growth factors (Amin et al., 2015). Especially in the stationary algal growth phase, Christie-Oleza et al. (2017) found that marine phototrophic cyanobacteria cultures are dependent on heterotrophic bacteria contaminants mainly due to their importance in degrading potentially toxic DOM exudates and regenerating ammonium. The current study aimed to bridge the gap between detailed representations of algae physiology and the role of microbial activity in an accurate way while keeping model complexity low.

Most ecosystem models consider only a single limiting nutrient to control primary production after Liebig's Law of the minimum (Wassmann et al., 2006; Vichi et al., 2007). Yet we know that nutrient co-limitation is more complex. For example, ammonium and glutamate can inhibit nitrate uptake (Morris, 1974; Dortch, 1990; Flynn et al., 1997), C and N uptake is reduced under Fe limitation, while Si uptake continues (Werner, 1977; Firme et al., 2003), and the effects on photosynthesis differs for nitrogen and silicon limitations and for different algal groups (Werner, 1977; Flynn, 2003; Hohn et al., 2009). Complex interaction models considering intracellular biochemistry (NH_4-NO_3 co-limitation, Flynn et al., 1997), transporter densities and mobility (Flynn et al., 2018), and cell cycles (Si limitation, Flynn, 2001) can accurately describe these dynamics (Flynn, 2003), but are ultimately too computationally expensive to be integrated and parameterized in large scale ecosystem models. Some models (Hohn et al., 2009, Le Quéré et al., 2016) implemented multinutrient (Hohn et al., 2009) and heterotrophic bacterial dynamics (Le Quéré et al., 2016) in Southern Ocean ecosystem models, but have their limitations in representing bacterial remineralisation (Hohn et al., 2009), or ammonium and silicate co-limitations (Le Quéré et al., 2016). In contrast to Antarctica, DIN is the primary limiting nutrient for phytoplankton growth while iron is not limiting in most Arctic systems (Tremblay and Gagnon, 2009; Moore et al., 2013).

While simple lab experiments cannot represent all nutrient dynamics found in the environment (e.g. N excretion by zooplankton), they can focus on the quantitatively most important dynamics, to facilitate the development of simple multinutrient models scalable to larger ecosystem models. The current study investigated the relevance of silicate, ammonium - nitrate co-limitation, bacterial nutrient regeneration and changes in photosynthesis, nitrogen assimilation, and cellular quotas in response to the changing nutrient limitations based on data from a culture based Arctic spring bloom system. The culture consisted of an axenic isolate of *Chaetoceros socialis*, dominating a phytoplankton net haul of a Svalbard fjord. The culture was used experimentally either under axenic conditions or after inoculation with bacteria cultures, isolated beforehand from the non-axenic culture. Parametrization and insights from these

incubations were then used to develop and parameterize a simple Carbon quota based dynamic model (based on Geider et al., 1998), aiming to keep the number of parameters, and computational costs low to allow its use in larger ecosystem models.

The aims of the study was I) to study the bloom dynamics of simplified Arctic coastal pelagic system in a culture experiment consisting of one Arctic diatom species and co-cultured bacteria, II) to develop a simple dynamic model representing the observed interactions, and III) to discuss the importance of more complex bloom dynamics and their importance for an accurate ecosystem model.

We hypothesize that: I) Bacterial regeneration extends a phytoplankton growth period and gross carbon fixation; II) Diatoms continue photosynthesis under silicate limitation at a reduced rate if DIN is available; III) Cultivation experiments are powerful for understanding the major spring bloom dynamics.

2 Methods

2.1 Cultivation experiment

The most abundant phytoplankton species from a net haul (20µm mesh size) in April 2017 in van Mijenfjorden (Svalbard) *Chaetoceros socialis* was isolated via the dilution isolation method (Andersen et al., 2005) on F/2 medium (Guillard, 1975). Bacteria were isolated on LB-medium (evaluated by Bertani, 2004) Agar plates using the algae culture as inoculum and sequenced at GENEWIZ LLC using the Sanger method and standard 16S rRNA primers targeting the V1-V9 region (Forwards 5'-AGAGTTTGATCCTGGCTCAG -3', Reverse 5'- ACGGCTACCTTGTTACGACTT -3') provided by GENEWIZ LLC for identification via blastn (Altschul et al., 1990). Two strains of *Pseudoalteromonas elyakovii*, a taxon previously isolated from the Arctic (Khudary et al., 2008) and known to degrade algae polysaccharides (Ma et al., 2008) and to excrete polymeric substances (Kim et al., 2016), were successfully isolated and used for the experiments. Before the start of the experiment, all bacteria in the algae culture were killed using a mixture of the antibiotics penicillin and streptomycin. The success was confirmed via incubation of the cultures on LB-Agar plates and bacterial counts after DAPI staining (Porter et al., 1980). The axenic cultures were diluted in fresh F/2 medium lacking nitrate addition (Guillard, 1975) using sterile filtered seawater of Tromsø sound (Norway) as basis. The algae cultures were transferred into 96 200ml sterile cultivation bottles with three replicates for each treatment. Half of the incubations were inoculated with bacteria cultures (BAC+), while the other half was kept axenic (BAC-). The cultures were incubated at 4°C and 100 µE m^{-2} s^{-1} continuous light and mixed 2-3 times a day to keep the algae and bacteria in suspension. We ensured sterile conditions during the experiment by keeping the cultivation bottles closed until sampling. However, endospores may survive the antibiotic treatment in low numbers and start growing especially towards the end of the experiment. Over 16 days three axenic and three BAC+ bottles were sacrificed daily for measurements of chlorophyll a (Chl), particulate organic carbon (POC) and nitrogen (PON), bacterial and algal abundances, nutrients (nitrate, nitrite, ammonium, phosphate, silicate), dissolved organic carbon (DOC), and the maximum quantum yield (QY) of PSII (Fv/Fm) as a measure of healthy photosystems.

Chlorophyll a was extracted from a GF/F (50ml filtered at 200mbar) filter at 4C° for 12-24h in 98% methanol in the dark before measurement in a Turner Trilogy™ Fluorometer (evaluated by Jacobsen and

Rai, 1990). POC and PON were measured after filtration onto precombusted (4h at 450°C) GF/F (Whatman) filters (50ml filtered at 200mbar), using a Flash 2000 elemental analyser (Thermo Fisher Scientific, Waltham, MA, USA) and Euro elemental analyser (Hekatech) following the protocol by Pella and Colombo (1973) after removing inorganic carbon by fuming with saturated HCl in a desiccator. Bacteria were counted after fixation of a water sample for 3-4h with 2% Formaldehyde (final concentration), filtration of 25ml on 0.2µm pore size Polycarbonate filter, washing with filtered Seawater and Ethanol, DAPI staining for 7 minutes after Porter et al. (1980), and embedding in Citifluor-Vectashield (3:1). Bacteria were counted in at least 20 grids under an epifluorescence microscope (Leica DM LB2, Leica Microsystems, Germany) at 10x100 magnification. In the same sample the average diameter of diatom cells at the start and end of the experiment was measured. Algae were counted in 2ml wells under an inverted microscope (Zeiss Primovert, Carl Zeiss AG, Germany) at 20x10 magnification after gentle mixing of the cultivation bottle. Algae cells incorporated in biofilms after day 9 in the BAC+ cultures were counted after sonication in a sonication bath until all cells were in suspension. Nutrient and DOC samples were sterile filtered (0.2µm) and stored at -20°C before measurements. Nutrients were measured in triplicates after using standard colorimetric on a nutrient analyser (QuAAtro 39, SEAL Analytical, Germany) using the protocols No. Q-068-05 Rev. 12 for nitrate (detection limit = 0.02 µmol L^{-1}), No. Q-068-05 Rev. 12 for nitrite (detection limit = 0.02 µmol L^{-1}), No. Q-066-05 Rev. 5 for silicate (detection limit = 0.07 µmol L^{-1}), and No. Q-064-05 Rev. 8 for phosphate (detection limit = 0.01 µmol L^{-1}). The data were analysed using the software AACE. The nutrient analyzer was calibrated with reference seawater (Ocean Scientific International Ltd., United Kingdom). Ammonium was measured manually using the colorimetric method after McCarthy et al., (1977) on a spectrophotometer (Shimadzu UV-1201, detection limit = 0.01 µmol L^{-1}). DOC was measured by high temperature catalytic oxidation (HTCO) using a Shimadzu TOC-5000 total C analyser following methods for seawater samples (Burdige and Homstead, 1994). The photosynthetic quantum yield was determined using an Aquapen PA-C 100 (Photon Systems Instruments, Czech Republic).

Certain factors, such as grazing, settling out of the euphotic zone, and bacterial and algae succession were not included into the experimental set-up to reduce complexity, and focus on nutrient dynamics. Trace metals, phosphate, and Vitamin B12 in coastal systems are assumed to be not limiting in Arctic coastal systems and were supplied in excess to the culture medium. Realistic pre-bloom DOC concentrations were present in the medium as it was prepared with sterilized seawater from the Fjord outside Tromsø before the onset of the spring bloom (March 2018).

All plots were done in R. The f-ratio as indication for the importance of regenerated production (Eppley, 1981) was calculated based on the average PON fixation in the last three days of the experiment (Eq C1). Here, nitrogen assimilation in the BAC- culture was assumed to be based on new (nitrate based) production, while fixation in the BAC+ experiment was assumed to also be based on regenerated (ammonium based) production.

2.2 Model structure

This section outlines the overall model structure followed by a description of the chosen parametrization approach for each relevant process. Details regarding model equations are provided in the Appendix (Table A1) and a schematic representation of the models is given in Figure 1. We used a dynamic cell

quota model by Geider et al. (1998) to describe the BAC- experiment (G98). We then extended the G98 model to represent the role of silicate limitation, bacterial regeneration of ammonium, and different kinetics for ammonium and nitrate uptake (EXT) and fitted it to the BAC+ experiment while retaining the parameter values estimated for G98.

The Geider et al. (1998) model (G98) describes the response of phytoplankton to different nitrogen and light conditions and is based on both intracellular quotas and extracellular dissolved inorganic nitrogen (DIN) concentrations, allowing decoupled C and N growth (Fig. 1). Within this model, light is a control of photosynthesis and chlorophyll synthesis. C:N ratios and DIN concentrations control nitrogen assimilation, which is coupled to chlorophyll synthesis and photosynthesis. Chl:N ratios are controlling photosynthesis and chlorophyll synthesis. G98 has been used in a variety of large scale ecosystem models with some extensions representing the actual conditions in the environment or mesocosms (e.g. Moore et al., 2004; Schartau et al., 2007; Hauck et al., 2013). Photoacclimation dynamics in Geider type models have been evaluated as quick and robust (Flynn et al., 2001), while the N-assimilation component has some shortcomings in regard to ammonium-nitrate interactions. The original model of Geider et al. (1998) for C and N was corrected for minor typographical errors (see Ross and Geider, (2009); Appendix Tables A6 A7).

One aim of the study was to develop a model (EXT) with simplified dynamics of nutrient co-limitation, which is suitable for future implementation in coupled biogeochemistry-circulation models. The EXT model keeps all formulations of the G98 and adds dynamics and interactions of silicate, nitrate and ammonium uptake, carbon and nitrogen excretion and bacterial remineralisation (Fig. 1). The aim of the model was to describe the response in photosynthesis, chlorophyll synthesis and nitrogen assimilation with a minimal number of parameters. Hence, dynamics in silicate cycling and bacterial physiology were highly simplified. The limitations of these simplifications and the potential need for more complex models are discussed later.

Silicate uptake was modelled using Monod kinetics after Spilling et al. (2010). The response of silicate limitation on photosynthesis and chlorophyll synthesis was implemented after findings by Werner (1978), Martin-Jézéquel et al. (2000), and Claquin et al. (2002). Werner (1978) found that silicate limitation can lead to a 80% reduction in photosynthesis and a stop of chlorophyll synthesis in diatoms within a few hours. Hence, we added a parameter for the reduction of photosynthesis under silicate limitation (Si_{PS}) and formulated a stop of chlorophyll synthesis under silicate limitations.

N and Si metabolism have different controls and intracellular dynamics, with N uptake fuelled by photosynthesis (as P_C^{ref} in G98) and Si mainly fuelled by heterotrophic respiration (Martin-Jezequel et al., 2000). Besides earlier cultivation studies, the reduction of photosynthesis after Si limitation has been shown via photophysiological (inhibited PSII reaction centre, Lippemeier et al., 1999) and molecular (down-regulated photosynthetic proteins, Thangaraj et al., 2019) approaches. In general, we assume that nitrogen metabolism is not directly affected by silicate limitation (Hildebrand 2002, Claquin et al., 2002), but we expect cellular ratios to be affected by reduced photosynthesis and chlorophyll synthesis under Si limitation (Hildebrand, 2002; Gilpin, 2004).

The algal respiration term included both respiration and excretion of dissolved organic nitrogen and carbon as a fraction of the carbon and nitrogen assimilated. For testing the importance of DON excretion we also ran the EXT model without DON excretion (EXT_{-excr}). Dissolved organic nitrogen (DON) was recycled into ammonium via bacterial remineralisation. It was assumed that this process is faster for

freshly excreted DON compared to DON already present in the medium. Thus, we implemented a labile (DON_l) and refractory (DON_r) DON pool with different remineralization rates (rem, rem_d). We also assumed that excreted DON and DOC do not coagulate as extracellular polymeric substances (EPS) during the course of the experiment. After Tezuka (1989), net bacterial regeneration of ammonium occurs at DOM C/N mass ratio below 10 and is proportional to bacterial abundances. Higher thresholds up to 29 have been found (e.g. Kirchmann, 2000), but we selected a lower number to stay conservative. DOM C/N ratios are assumed to be proportional to algae C/N ratios (van der Meersche et al., 2004), with algal C/N ratios below 10 representing substrate (DOM) C/N ratios below 10.5. Hence, we assume net bacterial ammonium regeneration to occur at POC/PON ratios below 10, while higher ratios lead to bacteria retaining more N for growth than they release. Bacteria abundance change was estimated using a simple logistic growth curve as a function of DOM since the number of parameters is low (2) and the fit sufficient for the purpose of modelling algae physiology. Michaelis-Menton kinetics based on bacteria growth on DOM with different labilities kinetics could give a more accurate representation of bacterial growth, but would not change the fit of the other model parameters aiming for the best fit of the model output to algal PON, POC, Chl, and DIN. Algal nitrate uptake was modelled after the original model by Geider et al. (1998) and ammonium assimilation was based on the simplified SHANIM model by Flynn and Fasham (1997b), excluding the internal nutrient and glutamine concentrations. Ammonium uptake is preferred over nitrate (lower half saturation constant) and reduces nitrate assimilation if available above a certain threshold concentration of ammonium (Dortch, 1990; Flynn, 1999). Ammonium is the primary product of bacterial regeneration N-compound after remineralization of DON. Nitrification was assumed to be absent, since the bacteria in our experiment are not known to be capable of nitrification.

2.3 Model fitting

The model was written as a function of differential equations in R. All model equations are provided in the Appendix (Table A6) and the R code is available in the supplement. The differential equations were solved using the ode function of the deSolve package (Soetart et al., 2010) with the 2nd-3rd order Runge-Kutta method with automated stepsize control. deSolve is one of the most widely used packages for solving differential equations in R.

Parameter of the G98 model were fitted to the BAC- experiment data and the EXT model was fitted to the BAC+ experiment data. The G98 parameter values were fitted first and retained without changes for the EXT model fitting. The maximum Chl:N ratio (θ^N_{max}), minimum and maximum N:C ratios (Q_{min}, Q_{max}), and irradiance (I) are given by the experimental data and needed no further fitting (Table A2). The start values and constraints for the remaining six variables (ζ, R^C, α_{Chl}, n, K_{no3}, P^C_{ref}, Table A3) were based on model fits of G98 to other diatom cultures in previous studies (Geider 1998, Ross and Geider 2009). The parameters were first fitted manually via graphical comparisons with the experimental data (POC, PON, Chl, DIN, Fig. 5 and 5), and via minimizing the model cost calculated as the root of the sum of squares normalized by dividing the squares with the variance (RMSE Eq. C2, Stow et al., 2009). The initial manual tuning approach allowed control of the model dynamics, considering potential problems with known limitations of the G98 model (e.g lag phase not modelled; Pahlow, 2005). The manual tuning also allowed obtaining good start parameters for the automated tuning approach and sensitivity/ collinearity analyses, which are sensitive to the start parameters.

After the manual tuning, an automated tuning approach was used to optimize the fits. The automated tuning was done using the FME package (Soetart et al., 2010b), a package commonly used for fitting dynamic and inverse models based on differential equations (i.e. deSolve) to measured data. The automated analyses were based on minimizing the model cost calculated as the sum of squares of the residuals (SSR, Fitted vs measured data). The experimental data were normalized so that all normalized data were in a similar absolute range of values. This involved increasing Chl and PON values by an order of magnitude while decreasing DIN (NH_4 + NO_3) data by one order of magnitude The data were not weighted, assuming equal data quality and importance. Prior to the automated fitting, parameters were tested for local sensitivity (SensFun) and collinearity, or parameter identifiability (collin; e.g. Wu et al., 2014). sensFun tests for changes in output variables at each time point based on local perturbations of the model parameter. The sensitivity is calculated as L1 and L2 norms (Soetart et al. 2009; Soetart et al., 2010b). The sensFun output is further used as input for the collinearity, or parameter identifiability analyses. Parameters were considered collinear and not identifiable in combination with a collinearity index higher than 20 (Brun et al., 2001). In this case, only the more sensitive parameter was used for further tuning. Eventually, R^C, K_{no3}, n, and α_{Chl} were subject to the automated tuning approach using the modfit function, based on minimizing the SSR within the given constraints. Parameters were first fitted using a Pseudorandom search algorithm (Price, 1977) to ensure a global optimum. The resulting parameters were then fine-tuned using the Nelder-Mead algorithm (Soetart et al., 2010b) for finding a local optimum. A model run with the new parameters was then compared to the initial model via graphical comparisons of the model fit to the experimental data, and via the RMSE value.

The parameter values obtained for the G98 fit to the BAC- experiment were retained without changes or further fitting in the EXT model. The additional parameters of the EXT model were then fitted to the BAC+ experimental data (POC, Chl, PON, DIN). The model was only fitted to total DIN, due to the potential uncertainties related to ammonium immobilization in the biofilm. In fact, a test run, fitting the EXT model to NO_3 and NH_4 separately lead to a substantially worse overall fit (RMSE=8.79). Otherwise, the data were not weighted. Since the aim of the study was to model the effects of silicate and bacteria on algae growth and not to develop an accurate model for bacteria biomass and silicate concentrations, the parameters μ_{bact}, $bact_{max}$, K_{si}, and V_{max} were only fitted to the corresponding data (Bacteria, Silicate) prior to fitting the other parameters of the EXT model. Bacterial growth parameters (μ_{bact}, $bact_{max}$) were fitted to the bacterial growth curve. Silicate related parameters (K_{si}, V_{max}) were constrained by the study of Werner (1978) and fitted to the measured silicate concentrations. The remaining parameters were subject to the tuning approach described for G98. Ammonium related parameters (K_{nh4}, $nh4_{thres}$) were constrained by measured ammonium concentrations, and constants available for other diatom taxa described by Eppley et al. (1969). Remineralization parameters for excreted (rem) and background (rem_d) DOM were constrained by the data with the limitation of rem > rem_d, assuming that the excreted DOM is more labile. The parameters related to the effect of silicate limitation on photosynthesis and chlorophyll production (s_{min}, Si_{PS}) were constrained by the study of Werner (1978) and fitted as described for G98. None of the added parameters were collinear/ unidentifiable or given by the measured data and thus retained for the automated tuning approach. Eventually, the 15 parameters (Table A3) were fitted against 160 data points (Table A1).

Due to the biofilm formation in the stationary phase of the BAC+ experiment, we tested three additional modelling approaches representing different dynamics in biofilms: i) DOC coagulation to EPS as part of

the POC pool (Schartau et al., 2007), ii) Increased DOM excretion in the stationary phase (e.g. Christie-Oleza et al., 2017), and iii) Increased bacterial regeneration in the biofilm due to closer contact between algae and bacteria (Equations in Table S1). However, we suggest that the photosynthesis reduction term Si_{PS} can give very similar model outputs, while being similarly or more sensitive. Thus, we tested the sensitivity of the added parameters of the three extended biofilm models in comparison to Si_{PS} by testing the magnitude of perturbations of Si_{PS} needed to reverse the effects of the added biofilm parameter (Fig. S1-3). In every case, the effects could be reversed with similar or less perturbations of Si_{PS}. The main effect of the biofilm that we could not model with the available data appears to be ammonium immobilization in the biofilm, either due to adsorption, accumulation in pockets, or conversion to ammonia due to the locally reduced pH caused by increased bacterial respiration. Model stability was estimated by extending the model run for 30 days, to test for unrealistic model dynamics (Fig. S4).

3 Results

3.1 Cultivation experiment

The concentrations of nitrate and silicate declined rapidly over the course of the experiment (Fig. 2). After eight days, silicate decreased to concentrations below 2 µmol L^{-1} a threshold known to limit diatom dominance in phytoplankton (Egge and Aksnes, 1992), while inorganic nitrogen (nitrate, nitrite, and ammonium) became limiting (<0.5 µmol L^{-1} , POC:PON >8-9 DIN:DIP<16) only in the BAC- culture. DIN:DIP ratios far below 16, or DIN concentrations below 2 µmol L^{-1} have been described as indication for DIN limitation (Pedersen and Borum, 1996), as well as POC:PON ratios >9 (Geider and La Roche, 2002). Phosphate was not potentially growth limiting with molar DIN to PO_4 ratios consistently far below 16 (Redfield, 1934) and concentrations around 15 µmol L^{-1}. Typically, phosphate concentrations below 0.3 µmol L^{-1} are considered limiting (e.g. Haecky and Andersson, 1999). Regeneration of ammonium and phosphate were important after eight days as seen by increasing concentrations of both nutrients and showed higher concentrations in the BAC+ experiments compared to the BAC- cultures (Fig. 2a,b). Ammonium concentrations were consistently higher, and nitrate was removed more slowly in the presence of bacteria, especially during the exponential phase. With the onset of the stationary phase in the BAC+ experiment, PO_4 and NH_4 concentrations doubled within 2 to 4 days and stayed high with variations in phosphate concentrations, while they stayed low in BAC-. With depletion of NO_3 in BAC+, NH_4 concentrations remained high, while PO_4 concentrations dropped. While not all ammonium measured is also available for algae growth, discussion of the dynamics (decrease in the start, increase with the onset of the stationary phase), especially if also shown in the EXT model, are still useful to understand multinutrient dynamics (e.g. regeneration). Considering the overall higher concentrations of NO_3, compared to NH_4, discussions of total DIN dynamics, DIN.DIP ratios, and limitations are also meaningful. DOC values were very high from the start (approx. 2-4 mmol L^{-1}) and remained largely constant throughout the experiment (Table A8).

The diatom *Chaetoceros socialis* grew exponentially in both treatments until day 8 before reaching a stationary phase with declining cell numbers (Fig. 3). The growth rate of the BAC- culture (0.36 d^{-1}) was slightly lower than in the treatment with bacteria present (0.42 d^{-1}) during the exponential phase. Algal

cellular abundance was higher in the BAC+ cultures. Towards the end of the exponential phase, the diatom started to form noticeable aggregates in cultures with bacteria present, but only to a limited extent in the BAC- cultures. Such aggregate formation with associated EPS production is typical for *C. socialis*. With the onset of the stationary phase in the BAC+ cultures about 30% of the cells formed biofilms on the walls of the cultivation bottles (estimated after sonication treatment). Bacteria (Fig. 3) continued to grow throughout the entire experiment, but growth rates slowed down from 0.9 to 0.6 after day 8. In the BAC- cultures, bacterial numbers increased after 8 days, but abundances remained two order of magnitude below the BAC+ cultures and effectively BAC- over the experimental incubation period. The maximum photosynthetic quantum yield (Fv/Fm) is commonly used as a proxy of photosynthetic fitness (high QY), indicating the efficiency of energy transfer after adsorption in photosystem II. Low values are typically related to stress, including for example nitrogen (Cleveland and Perry, 1987), or silicate (Lippemeier et al., 1999) limitation. We found an increase in QY from approx. 0.62 to 0.67 d^{-1} in the exponential phase and a decrease to approx. 0.62 in the BAC+ treatment after 8 days and to approx. 0.58 in the BAC- treatment (Table A8).

During algal exponential growth, POC and PON concentrations followed changes in algal abundances increasing four, seven, and 19-fold respectively, within 8 days (Fig. 3a, 4). Interestingly, with the beginning of the stationary phase, POC and PON continued to increase in the BAC+ cultures, while their concentrations stayed constant (POC), or decreased due to maintenance respiration (PON) in BAC- cultures. POC and PON concentrations were consistently higher (1.2 times POC, 1.4 times PON) in BAC+ cultures during the exponential phase. gC : gN ratios decreased in both cultures, but increased again after 11 days in the BAC- culture. Chlorophyll *a* concentrations also increased exponentially over the first eight days in both treatments, and thereafter decreased within the stationary phase in the BAC- cultures. In contrast, cell numbers remained nearly constant in the BAC+ cultures, before declining at the last sampling day.

Overall, both experimental cultures showed similar growth dynamics until day 8, with silicate becoming limiting for both treatments and nitrogen only limiting in BAC- cultures. Algal growth with bacteria present was slightly, but consistently higher during this phase. After eight days, algae growth stopped in both treatments, but nitrogen and carbon were continuously assimilated in BAC+ cultures. BAC- cultures started to degrade chlorophyll, while it stayed the same in BAC+ cultures. Algal abundances in the BAC+ treatment at the end of the experiment were ca 30% higher due to biofilm formation, and considerably more carbon (2x total POC, or 10-20% per cell) and nitrogen (3x total PON) per cell had been assimilated, and considerably more chlorophyll (2-3x total chlorophyll) produced at day 16. Cell size differences were not detectable (ca 4µm diameter, Table A8). POC to PON ratios increased after 11 days in BAC- cultures to maximum values of 7.2 and 1.3 mmol L^{-1}, respectively, but showed no change in BAC+ cultures. POC to Chl ratios were comparable in both treatments (Fig. 5). Assuming BAC- N fixation was mostly based on new production (nitrate as N source), while the algal N fixation in bacterial enriched treatments was based on new and regenerated (ammonium as N source) production, two-thirds of the production was based on regenerated production (f-ratio = 0.31).

3.2 Modelling

A comparison of the traditional G98 model with the EXT model allowed an estimate of importance of bacterial DIN regeneration and Si co-limitations for describing the experimental growth dynamics. The EXT model led to a slightly improved fit to the BAC- experiment ($RMSE_{G98}$ = 3.64 $RMSE_{EXT}$ = 3.34, Fig. 5 & 6). The real strength of the EXT model was in representing growth dynamics with bacteria present (Fig. 5 & 6). Here, the fitted lines mostly overlapped with the range of measured data and the RMSE was reduced by 55% from $RMSE_{G98}$ = 4.57 down to $RMSE_{EXT}$ = 2.12.

Both, the G98 and EXT model fits of the BAC- experiment were equally good for POC and PON with a slightly lower modelled growth rate. However, both models had limitations in modelling chlorophyll production, which was underestimated by about 20% at the onset of the stationary phase (Fig. 5c). The degradation of chlorophyll *a* in the stationary phase was not modelled either (Fig. 5c). PON in the BAC+ experiment was poorly modelled without consideration of silicate limitation or regenerated production specifically towards the end of the exponential phase and during the stationary phase. Maximum PON values were about 3 times lower using the G98 model (Fig. B3). In addition, the start of the stationary phase in the BAC+ experiment was estimated 3 days too late via G98, even though modelled DIN was depleted 2 days too soon (Fig. B3). Under BAC- conditions, where silicate limitation does not play a major role the G98 model appears sufficient.

The EXT model allowed representing detailed dynamics in a bacteria influenced system such as the responses to silicate limitation with a decrease in POC production, continued PON production, and the stagnation of Chl synthesis (Fig. 5). Apart from the lag phase, the mass ratios of C:N and C:Chl were represented accurately (Fig. 5). The model fits without the separate carbon excretion term (x_f) were overall similar to the model with excretion, indicating the importance of the high background dissolved organic matter (DOM) concentrations, rather than excreted DOM for the regenerated ammonium, and the lack of significant aggregation of excreted DOM ($RMSE_{EXT\text{-}exr}$ of 2.21).

DIN dynamics caused by ammonium – nitrate interactions were represented well (Fig. 6a). However, at the onset of the stationary phase, ammonium concentrations of the model were one order of magnitude lower than in the experiment, showing a major weakness (Fig. 6c). Increased weighting of ammonium during the model fitting led to a slightly better fit to ammonium, but a substantially worse fit of the model to POC, PON, and Chl ($RMSE_{EXT}$=8.79). This indicates that the problem lies with the ammonium data, which include immobilized ammonium in the biofilm, unavailable for diatoms growth, while the model assumes that all ammonium is available. Other potential differences in biofilms, were tested via different model extensions (DOC aggregation to EPS, increase DOM excretion, increased regeneration), but all dynamics (Table S1) could be explained by the Si_{PS} term of the EXT model (Fig. S1-3). The silicate uptake estimation was highly simplified using simple Monod kinetics, leading to too high modelled values in the stationary phase and a too quick depletion in the start (Fig. 6d). Carbon excretion (x_f) did not have any effect on the model fit to nutrients.

The sensitivity analysis (Fig. B1, Table A1) revealed that the sensitivity of the added parameters in EXT is overall comparable to the sensitivity of the original parameters in G98. The model outputs were most sensitive to P_C^{Ref} (L1=0.8, L2=1.5), which is a parameter in both G98 and EXT. The most sensitive added parameters in EXT were the remineralisation rate of refractory DON (rem_d, L1=0.24), the half saturation constant for ammonium (K_{nh4}, L1=0.08) and the inhibition of photosynthesis under Si limitation ($Si_{PS,}$

L1=0.08), which was comparable to other sensitive parameters of the G98 model (Q_{max}, R^C, α_{Chl}, ζ, n, I, Θ_N^{max}, Table A1). Small perturbations of the parameters only indirectly related to the fitted output variables did not lead to changes in POC, PON, Chl, or DIN.

4 Discussion

The experimental incubations represented typical spring bloom dynamics for coastal Arctic systems, including an initial exponential growth phase terminated by N and Si limitation and the potential for an extended growth period via regenerated production. Our model incorporating these results was able to reflect these dynamics by adding NH_4-NO_3-$Si(OH)_4$ co-limitations and bacterial NH_4 regeneration to the widely used G98 model. In addition, bacteria-algae interactions and DOC and biofilm dynamics were important in the experiment, but those were not crucial for quantitatively modelling algal C:N:Chl quotas. While *C. socialis* may not be the dominant species in all coastal Arctic phytoplankton blooms, we argue that it is representative for chain-forming diatoms typically dominating these systems due to their shared needs and responses to nutrient limitations (e.g. Eilertsen et al., 1989; von Quillfeldt, 2005).

4.1 Silicon-nitrogen regeneration

Spring phytoplankton dynamics in Arctic and sub-Arctic coastal areas is typically characterised by an initial exponential growth of diatoms, followed by peaks of other taxa (like *Phaeocystis pouchetii*) soon after the onset of silicate limitation (Eilertsen et al. 1989). Thus, a shift in species composition for the secondary bloom is linked to silicate limitation prior to final bloom termination caused by inorganic nitrogen limitation. Photosynthesis was reduced by approx. 70% after silicate became limiting, which is comparable to earlier experimental studies (Tezuka, 1989). However, the secondary bloom was extended in time by bacterial regeneration of ammonium, allowing regenerated production to contribute about 69% of the total production (f-ratio=0.31) even during the diatom dominated scenario in our experimental incubation. With the start of the stationary phase, NH_4 and PO_4 concentrations doubled, presumably due to decreased assimilation by the silicate starved diatoms and increased regeneration by bacteria, supplied with increasing labile DOM (doubled remineralisation rate in EXT) excreted by the stressed algae. After NO_3 depletion at day 15, also PO_4 concentrations drop, indicating a coupling of N:P metabolism. Excretion of organic phosphate by diatoms is also common in cultures with surplus orthophosphate (Admiraal and Werner, 1983), which can be another explanation of the phosphate peak after silicate becomes limiting. The presence of bacteria and thus regenerated production allowed diatom growth to continue 8 days after silicate became limiting (Figs. 2, 3 & 4), nearly doubling the growth period similar to observations in the field (e.g. Legendre and Rassoulzadegan, 1995; Johnson et al., 2007).

The G98 model has its most severe limitation, the modelling of PON, simply due to the lack of the ammonium pool, supplied via bacterial regeneration. The substantially better fit of PON in the EXT model shows therefore clearly that bacterial remineralisation is crucial to successfully model spring bloom dynamics, especially near bloom termination. Many biogeochemical models used in the Arctic include remineralisation, but rely on fixed or temperature dependent rates and do not consider them bacteria-dependent (MEDUSA, LANL, NEMURO, NPZD, see Table 1). While this simplification allows modelling regenerated production, using bacteria-independent remineralisation rates does have

limitations under spring bloom scenarios, where bacteria biomass can vary over orders of magnitudes (e.g. Sturluson et al., 2008) as also seen in our experimental study.

While we do not expect the f-ratio in our bottle experiment to be directly comparable to open ocean system, which does include a variety of algal taxa beyond *C. socialis*, a comparison can aid to identify limitations in our experiment and model. Regenerated production is significant in polar systems and our estimated experimental f-value of 0.31 is slightly below the average for polar systems (Harrison and Cota, 1990, mean f-ratio=0.54). Nitrification is a process supplying about 50% of the NO_3 used for primary production in the oceans, which may lead to a substantial underestimation of regenerated production (Yool et al., 2007), inflating the f-ratio interpreted as estimate for new production, potentially also in the study by Harrison and Cota (1990). The absence of vertical PON export in our experiment may be another explanation for the above average fraction of regenerated production. In the ocean environment, regenerated production is also affected by vertical export (sedimentation) and grazing which are not represented in the experimental incubations. Via sedimentation, a fraction of the bloom either in the form of direct algal sinking of fecal pellets is typically exported to deeper water layers, reducing the potential for N regeneration within the euphotic zone (e.g. Keck and Wassmann, 1996). Larger zooplankton grazing can lead to increased export of PON via fecal pellet aggregation, or diel vertical migration (Banse, 1995), but may also release ammonium and urea (Conover and Gustavson, 1999, Saiz et al., 2013).

In contrast, bacterial death by microflagellate grazing and viral lysis may supply additional nutrients, or DON available for N regeneration in the euphotic zone (e.g. Goldman and Caron, 1985), which potentially leads to an overestimation of regenerated production. Another potentially important N source for regenerated production may be urea (Harrison et al., 1985), which would lead to an even higher importance of regenerated production as suggested by our study. Hence, ecosystem scale models will need to consider these dynamics regarding bacterial abundances, microbial networks and particle export in addition to bacterial remineralization in order to model realistic ammonium regeneration in the euphotic zone.

Bacteria-mediated silicate regeneration is absent from the modelling approach, as indicated by the identical silicate concentrations in both treatments and models (Fig. 2). In the environment silicate dissolution is, in fact, mostly described as an abiotic process with temperature as the main control, and a minor contribution by bacterial remineralisation (Bidle and Azam, 1999). Our experiment indicates that silicate dissolution for *Chaetoceros socialis* was negligible at cold temperatures and the time scale of the incubations and typical for bloom durations and residence times of algae cells in the euphotic zone (Eilertsen et al., 1989, Keck and Wassmann, 1996). We conclude that silicate dissolution in coastal Arctic systems happens most likely in the sediment or deeper water layers and is only supplied via mixing in winter. In Antarctica substantial silicate dissolution has been observed but not in the upper 100 m, which has been related to the low temperatures (Nelson and Gordon, 1981) in agreement with our conclusion. Hence, modelling silicate regeneration in the euphotic zone is not necessary in these systems.

4.2 Algal growth response to Si and N limitation

The response of diatoms to Si or N limitation is based on different dynamics and different roles of N and Si in diatom growth. N is needed for proteins and nucleic acids and its uptake is mainly fueled by phototrophic reactions (Martin-Jézéquel et al., 2000). Si is only needed for frustule formation, mostly

during a specific time in the cell cycle (G2 and M phase, Hildebrand, 2002) and the assimilation mostly fueled by heterotrophic reactions (Martin-Jézéquel et al., 2000). Once N is limiting, growth rapidly stops (Geider et al. 1998). In the case of Si limitation, however, growth can continue with a slower rate if N is still available (Werner, 1978; Gilpin et al., 2004). Several studies found a reduced growth rate with weaker silicified cell walls (Hildebrand, 2002; Gilpin, 2004), but unaffected nitrogen assimilation under silicate limitation (Hildebrand 2002, Claquin et al., 2002) in accordance with our study. Claquin et al. (2002) found variable Si:C and Si:N ratios and highly silicified cells under nitrogen limitation, indicating uncoupled Si and N:C metabolism.

Nitrogen is a crucial element as part of amino acids and nucleic acids, which are necessary for cell activity and growth. If N becomes limiting major cellular processes are affected and growth or chlorophyll synthesis is not possible. Photosynthesis can continue for a while leading to carbon overconsumption (Schartau et al., 2007), which is well modelled by G98 for both BAC+ and BAC-. A part of the excess carbon can be stored as intracellular reserves, and a part is excreted as DOC, which may aggregate as EPS, contributing to the total POC pool. The excess carbon can potentially be toxic for the algae and excretion and extracellular degradation by bacteria may be crucial for algal survival (Christie-Oleza et al., 2017). Quantitatively, N limitation is well modelled by G98 under BAC- conditions, if only one nitrogen source plays a role. However, under longer nitrogen starvation times or higher light intensities, alternative models that include carbon excretion and aggregation (Schartau et al., 2007) or intracellular storage in reserve pools (Ross & Geider 2009) might be needed. Our growth experiment shows clearly, that C:N ratios are not fixed and variable quotas are needed. Vichi et al. (2007) estimated that Carbon based models may underestimate net primary production (NPP) by 50%, arguing for the importance of quota based models (Fransner et al., 2018). However, most ecosystem scale models are simplified by using fixed C:N ratios (Table 1). The next step to quota based-models is the consideration of more detailed cell based characteristics, such as transporter density, cell size, and mobility, including sedimentation (Aksnes and Egge, 1991). Flynn et al. (2018) discuss a model with detailed uptake kinetics showing that large cells are overall disfavored over small cells due to higher half saturation constants, but that they may still have competitive advantages due to lower investment in transporter production. Also increased sedimentation in larger cells increases the mobility and may offset the disadvantage of a larger size. While this extension is too complex for our aim of a simplified model, the dynamics may become important when modelling different algae taxa.

The type of inorganic nitrogen available also affects nitrogen uptake. Due to the metabolic costs related to intracellular nitrate reduction to ammonium, ammonium uptake is preferred over nitrate, potentially leaving more energy for other processes (Lachmann et al., 2019). Ammonium can even inhibit or reduce nitrate uptake over certain concentrations (Morris, 1974). The dynamics are mostly controlled by intracellular processes, such as glutamate feedbacks on nitrogen assimilation, cost for nitrate conversion to ammonium, or lower half saturation constants of ammonium transporters (Flynn et al., 1997). The most accurate representation of these dynamics are given in the ANIM model by Flynn et al. (1997), but the model is too complex for implementations in larger ecosystem models. The number of parameters is difficult to tune with the typically limited availability of measured data and its complexity makes it also computationally costly to scale the models up. Typically, modelling ammonium-nitrate interactions by different half-saturation constants and inhibition of nitrate uptake by ammonium appears sufficient (e.g. BFM, LANL, NEMURO, Table 1) and has been adapted in our model.

Studies on the coupling of silicate limitation on C, N, and Chl show inconclusive patterns, including a complete decoupling (Claquin et al., 2002), a relation of N to Si (Gilpin et al., 2004) and reduction of photosynthesis without new chlorophyll is production (Werner, 1978; Gilpin et al., 2004). Cell size is limited by the frustules, but cells may become more nutritious (higher N:C ratio), or simply excrete more DOM, which may aggregate and contribute to the PON and POC pools. A detailed cell-cycle based model has been suggested by Flynn (2001), but the number of parameters (30) makes the model too complex for ecosystem scale models. In ecosystem scale models Si limitation is modelled in various simplifications, such as thresholds triggering a stop (MEDUSA), or reduction (e.g. BFM, MEDUSA, SINMOD)of the Si dependent production (Table 1), or Si:N ratio scaled production (NEMURO, Table 1).

Our cultivation study shows i) that a threshold value in the model, leading to a stop or solely Si dependent photosynthesis has its limitations, since DIN controlled photosynthesis continues at lower rates, and ii) that coupling of Si:N:C:Chl is present. We do not expect a direct Si:N coupling, due to different controls of Si and N metabolism (Martin-Jézéquel et al., 2000.), but suggest indirect coupling via reduced photosynthesis. In fact, detailed photophysiological and molecular approaches under Si limitation found inhibited PSII reaction centers (Lippemeier et al., 1999) similar to the decreased QY in our experiment, and down-regulated photosynthetic proteins (Thangaraj et al., 2019) under Si limitation. Thus, we modelled the response of diatom growth to silicate limitation by reducing photosynthesis through a parameterized fraction (Si_{PS}) and a stop of chlorophyll synthesis below a certain threshold, based on experimental studies (Werner, 1978, Lippemeier et al., 1999, Gilpin et al., 2004, Thangaraj et al., 2019) and in accordance to other ecosystem scale approaches. Automated fitting showed the same 80 % reduction of photosynthesis as described by Werner (1978). We suggest that this extension is more accurate than the typical threshold based dynamics, with one limiting nutrient controlling the growth equally for POC and Chl production (e.g. SINMOD by Wassmann et al., 2006; BFM by Vichi et al., 2007), while still keeping the number of parameters low compared to very detailed cell-cycle based models (e.g. Flynn, 2001, Flynn et al., 2018).

4.3 Importance of algae-bacteria interactions and DOC excretion

As described above, N or Si limitation can lead to excretion of DON and DOC, which can aggregate as EPS and be available for bacterial regeneration of ammonium. For including EPS dynamics in the model additional data would be needed. However, the importance of EPS formation is clear in the end of the BAC+ experiment. Firstly, a biofilm was clearly visible containing about 30% of the algae cells. While we would not expect biofilms in the open ocean, aggregation of algae cells, facilitated by EPS is common towards the end of spring blooms, increasing vertical export fluxes (e.g. Thornton, 2002). *Chaetoceros socialis* is in fact a colony forming diatom building EPS-rich aggregates in nature (Booth et al., 2002). Secondly, POC and PON concentrations increased, while cell numbers and sizes stayed constant, showing that the additional POC and PON was most likely part of an extracellular pool. Silicate limitation could be one trigger for enhanced exudation. In fact, the three biofilm dynamics evaluated (DOC aggregation, increased excretion, increased regeneration) could all be modelled by the Si_{PS} term. Since the biofilm formation corresponds with silicate limitation, it is difficult to untangle the direct effects of the biofilm, or the indirect effects of silicate limitation, without additional data or experiments (e.g. EPS measurements, DOM characterization). However, only 30% of the culture was part of the biofilm and the

best fit of 80% reduction for the Si_{PS} term corresponds very well with an earlier study by Werner (1978), who did not have biofilm formation. Hence, we suggest that the main cause for the reduction of photosynthesis is related to Si limitation and not the biofilm.

Interestingly, algae – bacteria interactions can be species specific with specific organic molecules excreted by the algae to attract specific beneficial bacteria (Mühlenbruch et al., 2018). Thereby bacteria are crucial for recycling ammonium, but also to degrade potentially toxic exudates (Christie-Oleza et al., 2017).

In the BAC- experiment, Carbon excretion after Carbon overconsumption could be expected after Schartau et al. (2007), but no indications, such as biofilm formation, or increased POC per cell were found. This indicates that carbon overconsumption has been of minor importance likely due to the low light levels. An alternative explanation is that bacteria and potentially chemotaxis are important controls on algal carbon excretion (Mühlenbruch et al., 2018). Overall, DOM excretion and EPS dynamics appear to play a minor role in quantitatively modelling C:N:Chl quotas in our experiment, with similar $RMSE_{EXT-excr}$=2.21, $RMSE_{EXT}$=2.12) for a model run with and without the excretion term x_f. However, in systems with less allochthonous DOM inputs, such as open oceans compared to coastal sites, these dynamics will most likely play a more important role.

4.4 Considerations in a changing climate

Due to a rapid changing climate, especially in Arctic coastal systems, the dynamics addressed in this study will change (Tremblay and Gagnon 2009). With warmer temperatures, heterotrophic activities, and thereby bacterial recycling will increase (Kirchman et al., 2009). Our study showed that regenerated production is crucial for an extended spring bloom. Hence, higher heterotrophic activities may lead to extended blooms (increased bacterial regeneration). At the same time, higher temperatures and increased precipitation will lead to stronger and earlier stratified water columns, which will lead to less nutrients reaching the surface by winter mixing, reducing new production (decreased bacterial regeneration)(Tremblay and Gagnon, 2009; Fu et al., 2016). Consequently, the phenology of Arctic coastal primary production in a warmer climate will likely be increasingly driven by bacterial remineralization, showing the necessity to include this process into biogeochemical models. An earlier temperature driven water column stratification may also lead to an earlier bloom. However, due to increasing river and lake brownification and sediment resuspension, the spring bloom may also be delayed (Opdal et al., 2019). With decreased light, carbon overconsumption as described by Schartau et al. (2007) may become less important due to decreased photosynthesis. An earlier or later phytoplankton bloom can lead to a mismatch with zooplankton grazers (Durant et al., 2007; Sommer et al., 2007). Reduced zooplankton production would decrease the fecal pellet driven vertical export and thereby increase the residence time of POM in the euphotic zone and the potential for ammonium regeneration. Thus, the incorporation of bacterial recycling into ecosystem models may be even more important under this scenario. In fact, global climate change models agree that vertical carbon export is decreasing overall (Fu et al., 2016). Silicate regeneration is thought to be mostly controlled abiotically by temperature (Bidle and Azam, 1999). Thus, increasing temperature and a stronger stratification will allow recycling of silicate in the euphotic zone before sinking out and thus could cause a shift in the algal succession observed during spring with prolonged contributions of diatoms (Kamatani, 1982). Thus, a temperature dependent

silica dissolution may need to be included for models in a substantially warmer climate in further model developments. Increased precipitation will also lead to increased runoff and allochthonous DOM inputs, increasing the importance of terrestrial DOM degradation and decreasing the relative importance of algal exudate regeneration (Jansson et al., 2008). The high fraction of regenerated production mostly based on allochtonous DOM degradation, the limited role of excreted DOM degradation, low light levels, and the absence of grazing and export fluxes are simplifications of our study, which are, however, expected to be realistic scenarios under climate change. Hence, we suggest that our experiment and model are well suited as a baseline for predictive ecosystem models investigating the impacts of climate change on coastal Arctic spring blooms. However, climate change may lead to shifts in algae communities with non-silicifying algae dominating over diatoms (e.g. Falkowski and Oliver, 2007), reducing the importance of silicate limitation. Thus, conducting similar experiments and modelling exercises with a wider range of algal taxa and different temperature and nutrient regimes is suggested.

Acknowledgements

The project was supported by ArcticSIZE - A research group on the productive Marginal Ice Zone at UiT (project number 01vm/h15). We want to thank Paul Dubourg and Elzbieta Anna Petelenz-Kurdziel for the help with Nutrient and POC/PON analyses. DOC analyses was supported through a Fulbright Distinguished Scholar Award to HRH.

Authors contributions

TRV designed the experiment with contributions by RG and ML. TRV isolated and identified the cultures. ML performed the experiment with contributions of TRV and UD. RH measured DOC and SK measured the Nutrients. The other parameters where measured by ML and TRV. TRV programmed the model with contributions of CV, ST and DvO. TRV wrote the manuscript with contributions from all co-authors.

Data availability

The experimental data are archived at DataverseNO under the doi number doi.org/10.18710/VA4IU9. The Rscripts for the model are available at github under https://github.com/tvonnahm/Dynamic-Algae-Bacteria-model.

Competing interests

The authors declare that they have no conflict of interest.

References

Admiraal, W., and Werner, D.: Utilization of limiting concentrations of ortho-phosphate and production of extracellular organic phosphates in cultures of marine diatoms, Journal of plankton research, 5(4), 495-513, 1983.

Al Khudary, R., Stößer, N. I., Qoura, F., and Antranikian, G.: Pseudoalteromonas arctica sp. nov., an aerobic, psychrotolerant, marine bacterium isolated from Spitzbergen, Int. J. Syst. Evol. Microbiol., 58, 2018-2024, 2008.

Alcaraz, M., Almeda, R., Calbet, A., Saiz, E., Duarte, C. M., Lasternas, S., Agusti, S., Santiago, R., Movilla, J., and Alonso, A.: The role of arctic zooplankton in biogeochemical cycles: respiration and excretion of ammonia and phosphate during summer, Polar Biology, 33(12), 1719-1731, 2010.

Altschul, S. F., Gish, W., Miller, W., Myers, E. W. and Lipman, D. J.: Basic local alignment search tool, J. Mol. Biol., 215, 403-410, 1990.

Alver, M. O., Broch, O. J., Melle, W., Bagøien, E., and Slagstad, D.: Validation of an Eulerian population model for the marine copepod Calanus finmarchicus in the Norwegian Sea, Journal of Marine Systems, 160, 81-93, 2016.

Aksnes, D. L., and Egge, J. K.: A theoretical model for nutrient uptake in phytoplankton, Marine ecology progress series, 70(1), 65-72, 1991.

Amin, S. A., Parker, M. S., and Armbrust, E. V.: Interactions between diatoms and bacteria, Microbiol. Mol. Biol. Rev., 76(3), 667-684, 2012.

Amin, S. A., Hmelo, L. R., Van Tol, H. M., Durham, B. P., Carlson, L. T., Heal, K. R., Morales, R. L., Berthiaume, C. T., Parker, M. S., Djunaedi, B., Ingalls, A. E., Parsek, M. R., Moran, M. A., and Armbrust, E.V.: Interaction and signalling between a cosmopolitan phytoplankton and associated bacteria, Nature, 522, 98-101, 2015.

Andersen, R. A., and Kawachi, M.: Microalgae isolation techniques, in: Algal culturing techniques, edited by: Andersen, R. A., Elsevier, 83, 2005.

Anju, M., Sreeush, M. G., Valsala, V., Smitha, B. R., Hamza, F., Bharathi, G., and Naidu, C. V.: Understanding the Role of Nutrient Limitation on Plankton Biomass Over Arabian Sea Via 1-D Coupled Biogeochemical Model and Bio-Argo Observations, Journal of Geophysical Research: Oceans, 125(6), 2020.

Banse, K.: Zooplankton: pivotal role in the control of ocean production: I. Biomass and production, ICES J. Mar. Sci., 52, 265-277, 1995.

Bertani, G.: Lysogeny at mid-twentieth century: P1, P2, and other experimental systems, J. Bacteriol., 186, 595-600, 2004.

Bidle, K. D., and Azam, F.: Accelerated dissolution of diatom silica by marine bacterial assemblages, Nature, 397, 508-512, 1999.

Booth, B. C., Larouche, P., Bélanger, S., Klein, B., Amiel, D., and Mei, Z. P.: Dynamics of Chaetoceros socialis blooms in the North Water, Deep Sea Res. Part II Top. Stud. Oceanogr., 49, 5003-5025, 2002.

Brun, R., Reichert, P. and Kunsch, H. R.: Practical Identifiability Analysis of Large Environmental Simulation Models, Water Resour. Res. 37(4): 1015–1030, 2001.

Burdige, D.J., and Homstead, J.: Fluxes of dissolved organi carbon from Chesapeake Bay sediments. Geochim. Cosmochim. Acta, 58, 3407-3424, 1994.

Christie-Oleza, J. A., Sousoni, D., Lloyd, M., Armengaud, J., and Scanlan, D. J.: Nutrient recycling facilitates long-term stability of marine microbial phototroph–heterotroph interactions, Nat Microbiol, 2, 17100, 2017.

Claquin, P., Martin-Jézéquel, V., Kromkamp, J. C., Veldhuis, M. J. W., and Kraay, G. W.: Uncoupling of Silicon Compared With Carbon and Nitrogen Metabolisms and the Role of the Cell Cycle in Continuous Cultures of Thalassiosira Pseudonana (Bacillariophyceae) Under Light, Nitrogen, and Phosphorus Control, J. Phycol., 38(5), 922–930, 2002.

Cleveland, J. S., & Perry, M. J.: Quantum yield, relative specific absorption and fluorescence in nitrogen-limited Chaetoceros gracilis. Marine Biology, 94(4), 489-497, 1987.

Conover, R. J., and Gustavson, K. R.: Sources of urea in arctic seas: zooplankton metabolism, Marine Ecology Progress Series, 179, 41-54, 1999.

Degerlund, M., and Eilertsen, H. C.: Main species characteristics of phytoplankton spring blooms in NE Atlantic and Arctic waters (68–80 N), Estuaries Coast, 33, 242-269, 2010.

Dortch, Q.: The interaction between ammonium and nitrate uptake in phytoplankton. Mar. Ecol. Prog. Ser., Oldendorf, 61, 183-201, 1990.

Durant, J. M., Hjermann, D. Ø., Ottersen, G., and Stenseth, N. C.: Climate and the match or mismatch between predator requirements and resource availability, Climate research, 33, 271-283, 2007.

Egge, J. K., and Aksnes, D.L.: Silicate as regulating nutrient in phytoplankton competition, Mar. Ecol. Prog. ser., 83, 281-289, 1992.

Eilertsen, H. C., and Frantzen, S.: Phytoplankton from two sub-Arctic fjords in northern Norway 2002–2004: I. Seasonal variations in chlorophyll a and bloom dynamics, Mar. Biol. Res., 3, 319-332, 2007.

Eilertsen, H. C., Taasen, J. P., and WesIawski, J. M.: Phytoplankton studies in the fjords of West Spitzbergen: physical environment and production in spring and summer, J. Plankton Res., 11, 1245-1260, 1989.

Eppley, R. W., Rogers, J. N., and McCarthy, J. J.: Half-saturation constants for uptake of nitrate and ammonium by marine phytoplankton, Limnology and oceanography, 14(6), 912-920, 1969.

Eppley, R. W.: Autotrophic production of particulate matter, Analysis of marine ecosystems/AR Longhurst, 1981.

Falkowski, P. G., and Oliver, M. J.: Mix and match: how climate selects phytoplankton, Nat. Rev. Microbiol., 5, 813-819, 2007.

Field, C. B., Behrenfeld, M. J., Randerson, J. T., and Falkowski, P.: Primary production of the biosphere: integrating terrestrial and oceanic components, Science, 281, 237-240, 1998.

Firme, G. F., Rue, E. L., Weeks, D. A., Bruland, K. W., and Hutchins, D. A.: Spatial and temporal variability in phytoplankton iron limitation along the California coast and consequences for Si, N, and C biogeochemistry, Global Biogeochemical Cycles, 17(1), 2003.

Flynn, K. J.: A mechanistic model for describing dynamic multi-nutrient, light, temperature interactions in phytoplankton, J. Plankton Res., 23, 977-997, 2001.

Flynn, K. J.: Modelling multi-nutrient interactions in phytoplankton; balancing simplicity and realism, Prog. Oceanogr., 56, 249-279, 2003.

Flynn, K. J., and Fasham, M. J.: A short version of the ammonium-nitrate interaction model, J. Plankton Res., 19, 1881-1897, 1997.

Flynn, K. J., Fasham, M. J., and Hipkin, C. R.: Modelling the interactions between ammonium and nitrate uptake in marine phytoplankton. Philosophical Transactions of the Royal Society of London, Series B: Biological Sciences, 352, 1625-1645, 1997.
Flynn, K. J.: Nitrate transport and ammonium-nitrate interactions at high nitrate concentrations and low temperature, Mar. Ecol. Prog. Ser., 187, 283-287, 1999.
Flynn, K. J., Marshall, H., and Geider, R. J.: A comparison of two N-irradiance interaction models of phytoplankton growth, Limnol. Oceanogr., 46, 1794-1802, 2001.
Flynn, K. J., Skibinski, D. O., and Lindemann, C.: Effects of growth rate, cell size, motion, and elemental stoichiometry on nutrient transport kinetics, PLoS computational biology, 14(4), 2018.
Fransner, F., Gustafsson, E., Tedesco, L., Vichi, M., Hordoir, R., Roquet, F., Spilling, K., Kuznetsov, I., Eilola, K., Mörth, C., Humborg, C., and Nycander, J.; Non-Redfieldian Dynamics Explain Seasonal pCO2 Drawdown in the Gulf of Bothnia, J Geophys Res Oceans, 123, 166-188, 2017.
Fritz, M., Vonk, J. E., and Lantuit, H.: Collapsing arctic coastlines, Nat Clim Chang, 7, 6, 2017.
Fu, W., Randerson, J. T., and Moore, J. K.: Climate change impacts on net primary production (NPP) and export production (EP) regulated by increasing stratification and phytoplankton community structure in the CMIP5 models, Biogeosciences, 13, 5151-5170, 2016.
Geider, R., and La Roche, J.: Redfield revisited: variability of C: N: P in marine microalgae and its biochemical basis, European J. Phycol., 37(1), 1-17, 2002.
Geider, R. J., Maclntyre, H. L., and Kana, T. M.: A dynamic regulatory model of phytoplanktonic acclimation to light, nutrients, and temperature, Limnol. Oceanogr., 43, 679-694, 1998.
Gilpin, L.: The influence of changes in nitrogen: silicon ratios on diatom growth dynamics, J. Sea Res., 51, 21–35, 2004.
Goldman, J. C., and Caron, D. A.: Experimental studies on an omnivorous microflagellate: implications for grazing and nutrient regeneration in the marine microbial food chain, Deep Sea Res A, 32, 899-915, 1985.
Gruber, N., Frenzel, H., Doney, S. C., Marchesiello, P., McWilliams, J. C., Moisan, J. R., Oram, J. J., Plattner, G., and Stolzenbach, K. D.: Eddy-resolving simulation of plankton ecosystem dynamics in the California Current System, Deep Sea Research Part I: Oceanographic Research Papers, 53(9), 1483-1516, 2006.
Guillard, R.L.L.: Culture of phytoplankton for feeding marine invertebrates, in: Culture of Marine Invertebrates Animals, edited by: Smith, W.L., Chanley, M.H., Plenum Press, New York, 29–60, 1975.
Harrison, W. G., Head, E. J. H., Conover, R. J., Longhurst, A. R., and Sameoto, D. D.: The distribution and metabolism of urea in the eastern Canadian Arctic, Deep Sea Research Part A, Oceanographic Research Papers, 32(1), 23-42 1985.
Harrison, W. G., and Cota, G. F.: Primary production in polar waters: relation to nutrient availability, Polar Res, 10, 87-104, 1991
Haecky, P., & Andersson, A.: Primary and bacterial production in sea ice in the northern Baltic Sea, Aquat. Microb. Ecol., 20(2), 107-118, 1999.
Hauck, J., Völker, C., Wang, T., Hoppema, M., Losch, M., & Wolf-Gladrow, D. A.: Seasonally different carbon flux changes in the Southern Ocean in response to the southern annular mode, Global Biogeochem Cycles, 27, 1–10, 2013.

Henson, S. A., Cole, H. S., Hopkins, J., Martin, A. P., and Yool, A.: Detection of climate change-driven trends in phytoplankton phenology, Global Change Biology, 24(1), e101-e111, 2018.
Hildebrand, M.: Lack of coupling between silicon and other elemental metabolisms in diatoms, J. Phycol., 38, 841–843, 2002.
Hohn, S.: A model of the carbon:nitrogen:silicon stoichiometry of diatoms based on metabolic processes, PhD thesis, Universit¨at Bremen, Bremen, 43-57, 2009.
Hünken, M., Harder, J., and Kirst, G. O.: Epiphytic bacteria on the Antarctic ice diatom Amphiprora kufferathii Manguin cleave hydrogen peroxide produced during algal photosynthesis, Plant Biology, 10, 519-526, 2008.
Iversen, K. R., and Seuthe, L.: Seasonal microbial processes in a high-latitude fjord (Kongsfjorden, Svalbard): I. Heterotrophic bacteria, picoplankton and nanoflagellates, Polar Biol., 34, 731-749, 2011.
Jacobsen, T. R., and Rai, H.: Comparison of spectrophotometric, fluorometric and high performance liquid chromatography methods for determination of chlorophyll a in aquatic samples: effects of solvent and extraction procedures, Internationale Revue der gesamten Hydrobiologie und Hydrographie, 75, 207-217, 1990.
Jansson, M., Hickler, T., Jonsson, A. and Karlsson, J.: Links between terrestrial primary production and bacterial production and respiration in lakes in a climate gradient in subarctic Sweden, Ecosystems, 11, 367–376, 2008.
Johnson, M., Sanders, R., Avgoustidi, V., Lucas, M., Brown, L., Hansell, D., Moore, M., Gibb, S., Liss, P., and Jickells, T.: Ammonium accumulation during a silicate-limited diatom bloom indicates the potential for ammonia emission events, Mar Chem, 106, 63-75, 2007.
Kamatani, A.: Dissolution rates of silica from diatoms decomposing at various temperatures, Mar. Biol., 68, 91– 96, 1982.
Keck, A., and Wassmann, P.: Temporal and spatial patterns of sedimentation in the subarctic fjord Malangen, northern Norway, Sarsia, 80, 259-276, 1996.
Kim, S. J., Kim, B. G., Park, H. J., and Yim, J. H.: Cryoprotective properties and preliminary characterization of exopolysaccharide (P-Arcpo 15) produced by the Arctic bacterium Pseudoalteromonas elyakovii Arcpo 15, Prep. Biochem. Biotechnol., 46, 261-266, 2016.
Kirchman, D. L.: Uptake and regeneration of inorganic nutrients by marine heterotrophic bacteria, Microbial ecology of the oceans, 2000.
Kirchman, D. L., Morán, X. A. G., and Ducklow, H.: Microbial growth in the polar oceans—role of temperature and potential impact of climate change, Nat. Rev. Microbiol., 7, 451-459, 2009.
Kishi, M. J., Kashiwai, M., Ware, D. M., Megrey, B. A., Eslinger, D. L., Werner, F. E., Noguchi-Aita, M., Azumaya, T., Fujii, M., Hashimoto, S., Huang, D., Iizumi, H., Ishida, Y., Kang, S., Kantakov, G. A., Kim, H., Komatsu, K., Navrotsky, V. V., Smith, S. L., Tadokoro, K., Tsuda, A., Yamamura, O., Yamanaka, Y., Yokouchi, K., Yoshie, N., Zhang, J., Zuenko, Y. I., and Zvalinsky, V. I.: NEMURO – a lower trophic level model for the North Pacific marine ecosystem, Ecol. Model., 202, 12–25, 2007.
Krause, J. W., Schulz, I. K., Rowe, K. A., Dobbins, W., Winding, M. H., Sejr, M. K., Duarte, C. M.,. and Agustí, S.: Silicic acid limitation drives bloom termination and potential carbon sequestration in an Arctic bloom, Sci Rep, 9(1), 1-11, 2019.
Lachmann, S. C., Mettler-Altmann, T., Wacker, A., & Spijkerman, E.: Nitrate or ammonium: Influences of nitrogen source on the physiology of a green alga, Ecology and evolution, 9(3), 1070-1082, 2019.

Lannuzel, D., Tedesco, L., Van Leeuwe, M., Campbell, K., Flores, H., Delille, B., Miller, L., Stefels, J., Assmy, P., Bowman, J., Brown, K., Castellani, G., Chierici, M., Crabeck, O., Damm, E., Else, B., Fransson, A., Fripiat, F., Geilfus, N, Jacques, C., Jones, E., Kaartokallio, H., Kotovitch, M., Meiners, K., Moreau, S., Nomura, D., Peeken, I., Rintala, J., Steiner, N., Tison, J., Vancoppenolle, M., van der Linden, F., Vichi, M., and Wongpan, P.: The future of Arctic sea-ice biogeochemistry and ice-associated ecosystems, Nature Climate Change, 1-10, 2020.

Le Quéré, C., Andrew, R. M., Canadell, J. G., Sitch, S., Korsbakken, J. I., Peters, G. P., Manning, A. C., Boden, T. A., Tans, P. P., Houghton, R. A., Keeling, R. F., Alin, S., Andrews, O. D., Anthoni, P., Barbero, L., Bopp, L., Chevallier, F., Chini, L. P., Ciais, P., Currie, K., Delire, C., Doney, S. C., Friedlingstein, P., Gkritzalis, T., Harris, I., Hauck, J., Haverd, V., Hoppema, M., Klein Goldewijk, K., Jain, A. K., Kato, E., Körtzinger, A., Landschützer, P., Lefèvre, N., Lenton, A., Lienert, S., Lombardozzi, D., Melton, J. R., Metzl, N., Millero, F., Monteiro, P. M. S., Munro, D. R., Nabel, J. E. M. S., Nakaoka, S.-I., O'Brien, K., Olsen, A., Omar, A. M., Ono, T., Pierrot, D., Poulter, B., Rödenbeck, C., Salisbury, J., Schuster, U., Schwinger, J., Séférian, R., Skjelvan, I., Stocker, B. D., Sutton, A. J., Takahashi, T., Tian, H., Tilbrook, B., van der Laan-Luijkx, I. T., van der Werf, G. R., Viovy, N., Walker, A. P., Wiltshire, A. J., and Zaehle, S.: Global carbon budget 2016, Earth Syst Sci Data, 8(2), 605-649, 2016.

Legendre, L., and Rassoulzadegan, F.: Plankton and nutrient dynamics in marine waters, Ophelia, 41, 153-172, 1995

Lippemeier, S., Hartig, P., and Colijn, F.: Direct impact of silicate on the photosynthetic performance of the diatom Thalassiosira weissflogii assessed by on-and off-line PAM fluorescence measurements, Journal of Plankton Research, 21(2), 1999.

Loebl, M., Colijn, F., van Beusekom, J. E., Baretta-Bekker, J. G., Lancelot, C., Philippart, C. J., Rousseau, V., and Wiltshire, K. H.: Recent patterns in potential phytoplankton limitation along the Northwest European continental coast, J. Sea Res., 61, 34-43, 2009.

Ma, L. Y., Chi, Z. M., Li, J., and Wu, L. F.: Overexpression of alginate lyase of Pseudoalteromonas elyakovii in Escherichia coli, purification, and characterization of the recombinant alginate lyase, World J. Microbiol. Biotechnol., 24, 89-96, 2008.

Martin-Jézéquel, V., Hildebrand, M., and Brzezinski, M. A.: Silicon Metabolism in Diatoms : Implications for Growth, J. Phycol., 36, 821–840, 2000.

Mills, M. M., Brown, Z. W., Laney, S. R., Ortega-Retuerta, E., Lowry, K. E., Van Dijken, G. L., and Arrigo, K. R.: Nitrogen limitation of the summer phytoplankton and heterotrophic prokaryote communities in the Chukchi Sea, Frontiers in Marine Science, 5, 362, 2018.

Moore, J. K., Doney, S. C., and Lindsay, K.: Upper ocean ecosystem dynamics and iron cycling in a global three-dimensional model, Global Biogeochem Cycles, 18, 2004.

Moore, C. M., Mills, M. M., Arrigo, K. R., Berman-Frank, I., Bopp,L., Boyd, P. W., Galbraith, E. D., Geider, R. J., Guieu, C., Jac-card, S. L., Jickells, T. D., La Roche, J., Lenton, T. M., Ma-howald, N. M., Maranon, E., Marinov, I., Moore, J. K., Nakat-suka, T., Oschlies, A., Saito, M. A., Thingstad, T. F., Tsuda, A.,and Ulloa, O.: Processes and patterns of oceanic nutrient limitation, Nat Geosci, 6, 701-710, 2013.

Morris, I.: Nitrogen assimilation and protein synthesis, Algal physiology and biochemistry, 10, 1974.

Mühlenbruch, M., Grossart, H. P., Eigemann, F., and Voss, M.: Mini-review: Phytoplankton-derived polysaccharides in the marine environment and their interactions with heterotrophic bacteria, Environ. Microbiol., 20, 2671-2685, 2018.

Nelson, D. M., & Gordon, L. I.: Production and pelagic dissolution of biogenic silica in the Southern Ocean, Geochim. Cosmochim. Acta, 46(4), 491-501, 1982.

Nelson, D. M., Treguer, P., Brzezinski, M. A., Leynaert, A., and Queguiner, B.: Production and dissolution of biogenic silica in the ocean: revised global estimates, comparison with regional data and relationship to biogenic sedimentation, Glob. Biogeochem. Cycles, 9, 359–372, 1995.

Opdal, A. F., Lindemann, C., and Aksnes, D. L.: Centennial decline in North Sea water clarity causes strong delay in phytoplankton bloom timing, Global change biology, 25(11), 3946-3953, 2019.

Pahlow, M.: Linking chlorophyll-nutrient dynamics to the Redfield N: C ratio with a model of optimal phytoplankton growth, Marine Ecology Progress Series, 287, 33-43, 2005.

Pedersen, M. F., and Borum, J.: Nutrient control of algal growth in estuarine waters. Nutrient limitation and the importance of nitrogen requirements and nitrogen storage among phytoplankton and species of macroalgae, Mar. Ecol. Prog. Ser., 142, 261-272, 1996

Pella E, Colombo B. Study of carbon, hydrogen and nitrogen determination by combustion-gas chromatography, Microchim Acta. 61, 697–719, 1973.

Ratkova, T. N., Wassmann, P.: Seasonal variation and spatial distribution of phyto- and protozooplankton in the central Barents Sea, Journal of Marine Systems, 38, 47-75, 2002.

Redfield, A. C.: On the proportions of organic derivatives in sea water and their relation to the composition of plankton, James Johnstone memorial volume, 176-192, 1934.

Rey, F., Skjoldal, H. R.: Consumption of silicic acid below the euphotic zone by sedimenting diatom blooms in the Barents Sea. MEPS, 36, 307-312, 1987.

Ross, O. N., and Geider, R. J.: New cell-based model of photosynthesis and photo-acclimation: accumulation and mobilisation of energy reserves in phytoplankton, Mar. Ecol. Prog. Ser., 383, 53-71, 2009.

Saiz, E., Calbet, A., Isari, S., Anto, M., Velasco, E. M., Almeda, R., Movilla, J., and Alcaraz, M.: Zooplankton distribution and feeding in the Arctic Ocean during a Phaeocystis pouchetii bloom, Deep Sea Research Part I: Oceanographic Research Papers, 72, 17-33, 2013.

Schartau, M., Engel, A., Schröter, J., Thoms, S., Völker, C., and Wolf-Gladrow, D.: Modelling carbon overconsumption and the formation of extracellular particulate organic carbon, Biogeosciences, 4, 13-67, 2007.

Schourup-Kristensen, V., Wekerle, C., Wolf-Gladrow, D., and Völker, C.: Arctic Ocean biogeochemistry in the high resolution FESOM 1.4-REcoM2 model, Progress in Oceanography, 168, 65-81, doi:10.1016/j.pocean.2018.09.006, 2018.

Slagstad, D., Wassmann, P. F., and Ellingsen, I.: Physical constrains and productivity in the future Arctic Ocean, Front Mar Sci, 2, 85, 2015.

Smith, K. M., Kern, S., Hamlington, P. E., Zavatarelli, M., Pinardi, N., Klee, E. F., and Niemeyer, K. E.: BFM17 v1. 0: Reduced-Order Biogeochemical Flux Model for Upper Ocean Biophysical Simulations, Geoscientific Model Development Discussions, 1-35, 2020.

Soetaert, K. and Herman, P. M. J.: A Practical Guide to EcologicalModelling -- Using R as a Simulation Platform, Springer, 390 pp, 2009.

Soetaert, K., Petzoldt, T.: Inverse Modelling, Sensitivity and Monte Carlo Analysis in R Using Package FME, J Stat Softw, 33, 1–28, doi: 10.18637/jss.v033.i03, 2010.
Soetaert, K., Petzoldt, T., and Setzer, R. W.: Solving Differential Equations in R: Package deSolve, J Stat Softw, 33, 1548-7660, doi: 10.18637/jss.v033.i09, 2010.
Sommer, U., Aberle, N., Engel, A., Hansen, T., Lengfellner, K., Sandow, M., Wohlers, J., Zollner, E., and Riebesell, U.: An indoor mesocosm system to study the effect of climate change on the late winter and spring succession of Baltic Sea phyto-and zooplankton, Oecologia, 150, 655-667, 2007.
Spilling, K., Tamminen, T., Andersen, T., and Kremp, A.: Nutrient kinetics modeled from time series of substrate depletion and growth: dissolved silicate uptake of Baltic Sea spring diatoms, Marine biology, 157, 427-436, 2010
Stow, C. A., Jolliff, J., McGillicuddy Jr, D. J., Doney, S. C., Allen, J. I., Friedrichs, M. A., Kenneth, A. R., and Wallhead, P.: Skill assessment for coupled biological/physical models of marine systems, J Mar Syst, 76, 4-15, 2009.
Sturluson, M., Nielsen, T. G., and Wassmann, P.: Bacterial abundance, biomass and production during spring blooms in the northern Barents Sea, Deep Sea Res. Part II Top. Stud. Oceanogr., 55, 2186-2198, 2008.
Sverdrup.H.U.: On conditions for the vernal blooming of phytoplankton, Cons. Perm. Int. Expl. Mer, 18, 287-295, 1953.
Teeling, H., Fuchs, B. M., Becher, D., Klockow, C., Gardebrecht, A., Bennke, C. M., Kassabgy, M., Huang, S., Mann, A. J., Waldmann, J., Weber, M., Klindworth, A., Otto, A., Lange,J., Bernhardt, J., Reinsch, C., Hecker, M., Peplies, J., Bockel-mann, F. D., Callies, U., Gerdts, G., Wichels, A., Wiltshire, K.H., Glöckner, F. O., Schweder, T., and Amann, R.: Substrate-controlled succession of marine bacterioplankton populations induced by a phytoplankton bloom, Science, 336, 608-611, 2012.
Teeling, H., Fuchs, B. M., Bennke, C. M., Krueger, K., Chafee, M., Kappelmann, L., Reintjes, G., Waldmann, J., Quast, C., Glöckner, F. O., Lucas, J., Wichels, A., Gerdts, G., Wiltshire, K. H., Amann, R.: Recurring patterns in bacterioplankton dynamics during coastal spring algae blooms, Elife, 5, 2016.
Tezuka, Y.: The C: N: P ratio of phytoplankton determines the relative amounts of dissolved inorganic nitrogen and phosphorus released during aerobic decomposition, Hydrobiologia, 173, 55-62, 1989.
Thangaraj, S., Shang, X., Sun, J., and Liu, H.: Quantitative proteomic analysis reveals novel insights into intracellular silicate stress-responsive mechanisms in the diatom Skeletonema dohrnii, International Journal of Molecular Sciences, 20(10), 2540, 2019.
Thornton, D.: Diatom aggregation in the sea: mechanisms and ecological implications, European Journal of Phycology, 37(2), 149-161, 2002.
Tremblay, J. É., and Gagnon, J.: The effects of irradiance and nutrient supply on the productivity of Arctic waters: a perspective on climate change, in: Influence of climate change on the changing arctic and sub-arctic conditions, edited by: Nihoul, J. C., J., Kostianoy, A. G., Springer, Dordrecht, 73-93, 2009.
Uitz, J., Claustre, H., Gentili, B., and Stramski, D.: Phytoplankton class-specific primary production in the world's oceans: Seasonal and interannual variability from satellite observations, Global Biogeochem Cycles, 24, 2010.
Van den Meersche, K., Middelburg, J. J., Soetaert, K., Van Rijswijk, P., Boschker, H. T., and Heip, C. H.: Carbon-nitrogen coupling and algal-bacterial interactions during an experimental bloom: Modeling a 13C tracer experiment, Limnol. Oceanogr., 49, 862-878, 2004.

Vichi, M., Pinardi, N., and Masina, S.: A generalized model of pelagic biogeochemistry for the global ocean ecosystem. Part I: Theory, J Mar Syst, 64, 89-109, 2007.

von Quillfeldt, C. H.: Common Diatom Species in Arctic Spring Blooms: Their Distribution and Abundance, Botanica Marina, 43(6), 499-516, https://doi.org/10.1515/BOT.2000.050, 2005.

Wassmann, P., Slagstad, D., Riser, C. W., and Reigstad, M.: Modelling the ecosystem dynamics of the Barents Sea including the marginal ice zone: II. Carbon flux and interannual variability, J Mar Syst, 59, 1-24, 2006.

Weitz, J. S., Stock, C. A., Wilhelm, S. W., Bourouiba, L., Coleman, M. L., Buchan, A., Follows, M.J., Fuhrman, J. A., Jover, L., Lennon, J. T., Middelboe, M., Sonderegger, D. L., Suttle, C. A., Taylor, B. P.,Thingstad, T. F., Wilson, W., and Wommack, K. E.: A multitrophic model to quantify the effects of marine viruses on microbial food webs and ecosystem processes, ISME J, 9, 1352-1364, 2015.

Werner, D.: Silicate metabolism, in: The biology of diatoms, edited by: Werner, D., Blackwell Scientific Publications, California, 13, 111-149, 1977.

Werner, D.: Regulation of metabolism by silicate in diatoms, in: Biochemistry of silicon and related problems, edited by: Bendz, G., and Lindqvist, I., Springer, Boston, MA, 149-176, 1978.

Westberry, T. K., Behrenfeld, M. J., Siegel, D. A., Boss, E.: Carbon-based primary productivity modeling with vertically resolved photoacclimation, Global Biogeochem Cycles, 22,1–18, 2008.

Wu, Y., Liu, S., Huang, Z., and Yan, W.: Parameter optimization, sensitivity, and uncertainty analysis of an ecosystem model at a forest flux tower site in the United States, Journal of Advances in Modeling Earth Systems, 6(2), 405-419, 2014.

Yool, A., Martin, A. P., Fernández, C., and Clark, D. R.: The significance of nitrification for oceanic new production, Nature, 447(7147), 999-1002, 2007.

Yool, A., and Popova, E. E.: Medusa-1.0: a new intermediate complexity plankton ecosystem model for the global domain, Geosci Model Dev, 4, 381, 2011.

Zambrano, J., Krustok, I., Nehrenheim, E., and Carlsson, B.: A simple model for algae-bacteria interaction in photo-bioreactors, Algal Res, 19, 155-161, 2016.

Figures

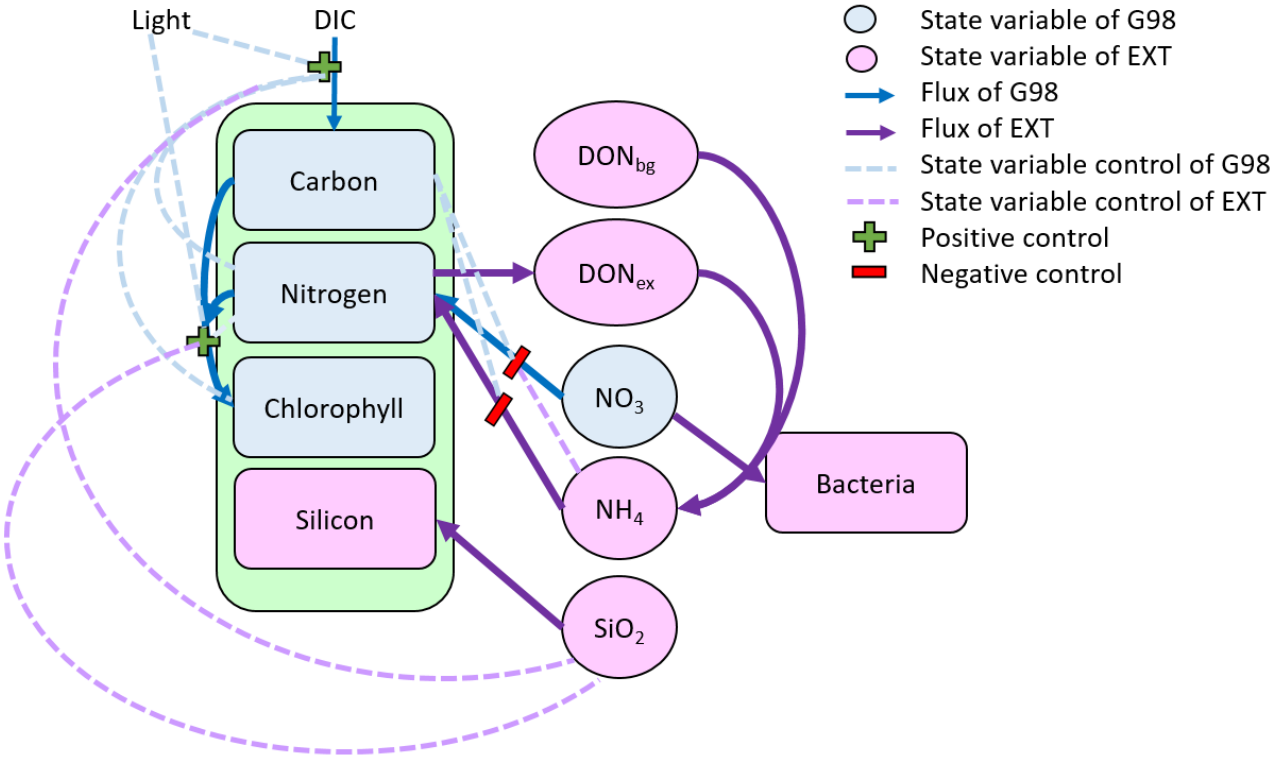

Figure 1. Schematic representation of the state variables and connections and controls in the G98 model (blue) and EXT model (purple). The EXT model has the same formulations as G98 with the additions shown in purple.

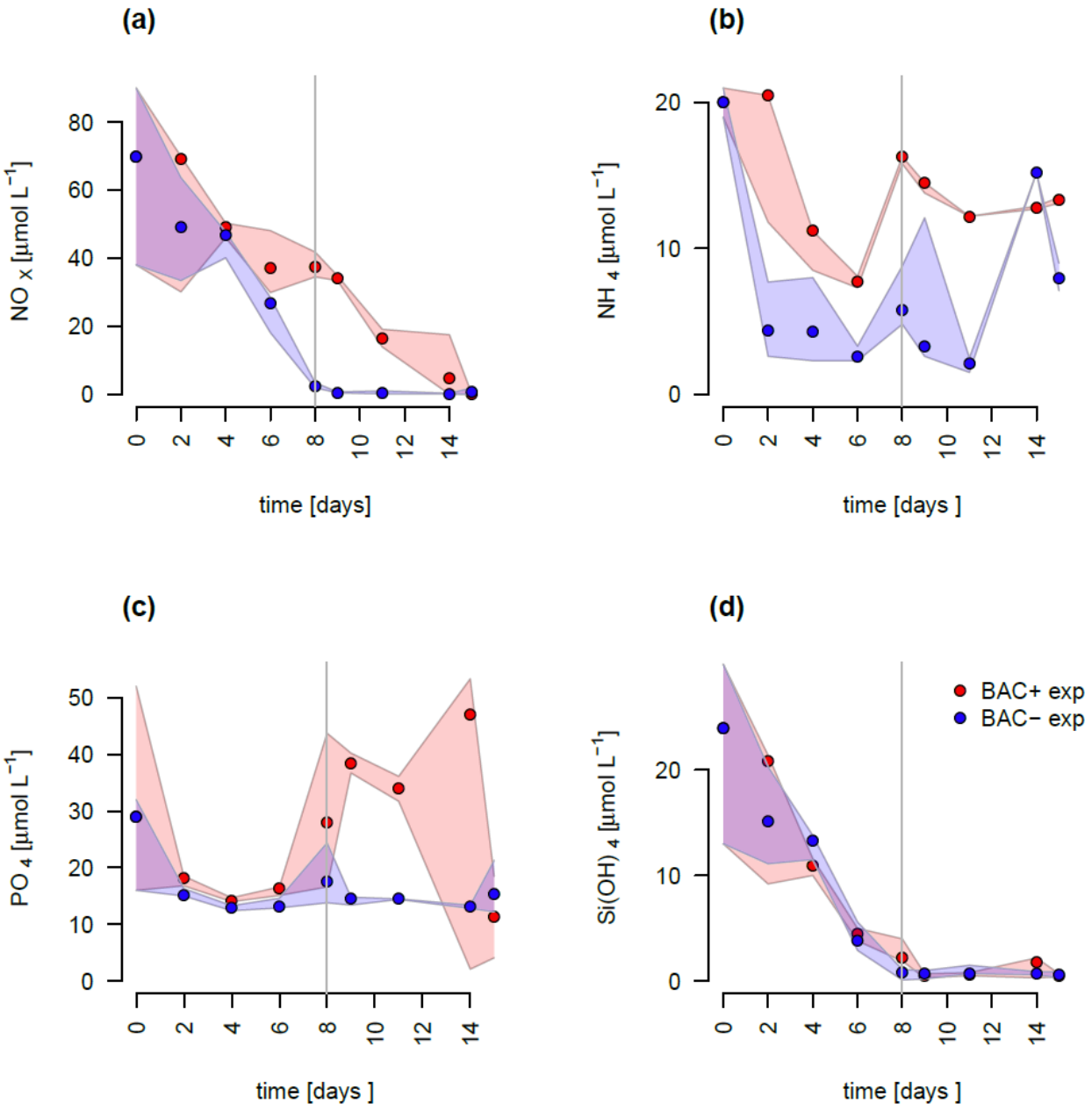

995 Figure 2. Nutrient measurements over the experimental incubations of a) NO_x, (NO_3^- + NO_2^-) b) NH_4^+, c) PO_4^{2-} with a potential outlier at day 14 leading to a negative peak, d) Silicate, red circles are BAC- cultures and green symbols are BAC+ cultures. Circles show median values (blue = BAC-, red = BAC+) and the colored polygons show maximum and minimum of measured data (n=3). The grey line shows the beginning of the stationary growth phase of *Chaetoceros socialis*.

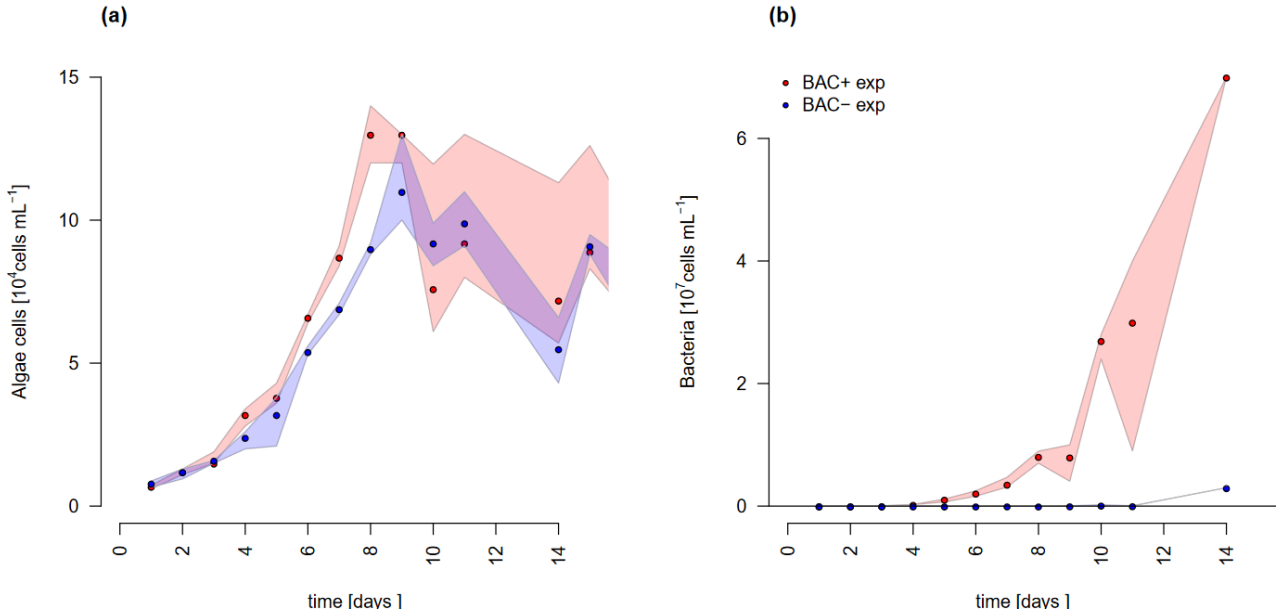

Figure 3. Abundances of a) *Chaetoceros socialis* and b) bacteria over the 14 day experimental period. Blue data are from BAC- cultures and red from BAC+ cultures. Circles represent median values (blue= BAC-, red = BAC+) and the colored polygons show maximum and minimum of measured data (n=3) (Not visible for bacteria counts in BAC- cultures due to very small range). The maximum values of the BAC+ experiment includes algae cells in the biofilm (after day 9).

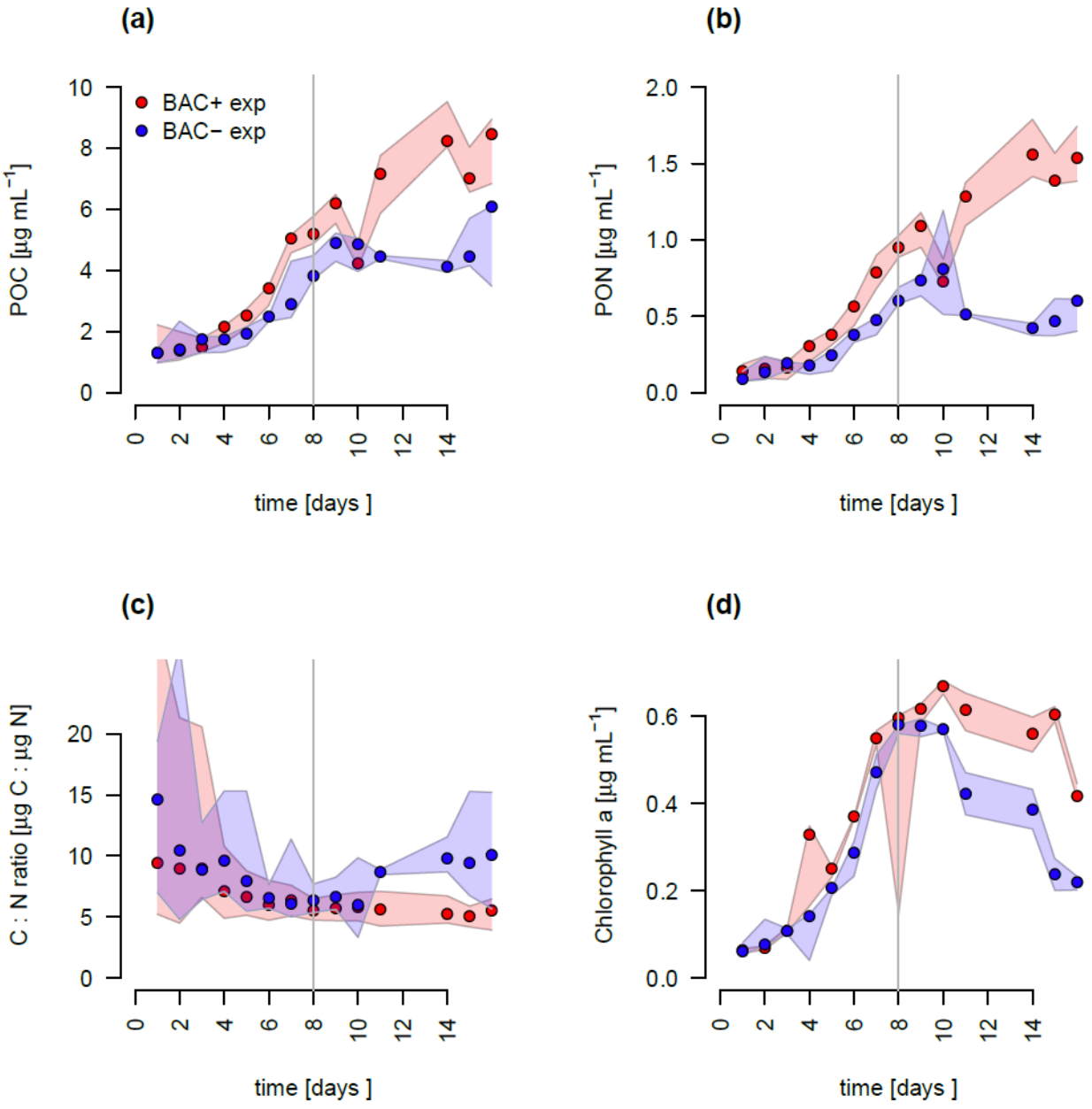

Figure 4. Total particulate organic a) Carbon (POC) b) Nitrogen (PON), c) C : N ratios, and d) Chlorophyll a concentration in experimental cultures with a potential outlier at day 8, presumably due to photodegradation, causing a negative spike. Blue symbols are BAC- cultures and red show BAC+ cultures. Circles show median values (blue = BAC-, red = BAC+) and the colored polygons show the maximum and minimum of measured data (n=3). The grey line indicates the start of the stationary phase.

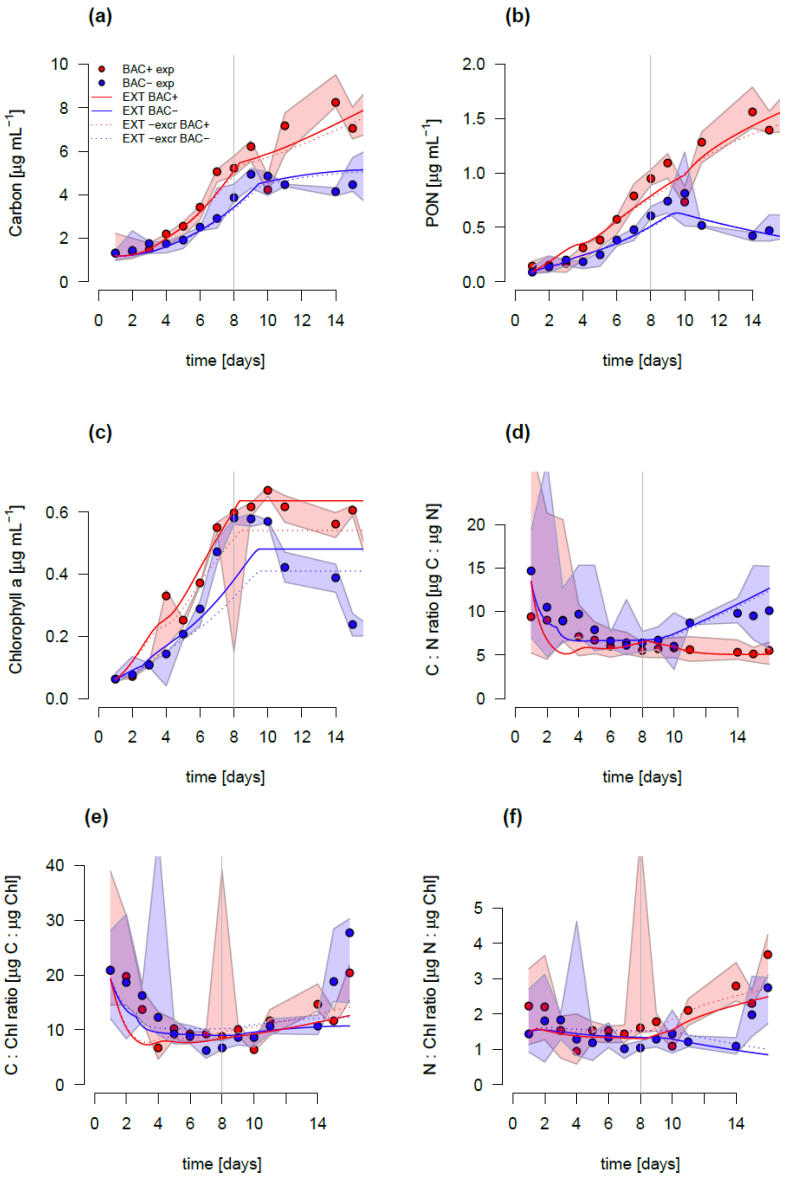

Figure 5. Model fit of the EXT model to the BAC- (blue) and BAC+ (red) experiment. Circles show median values and the colored polygons show the maximum and minimum of measured data (n=3). Solid lines show the model outputs of a) POC, b) PON, c) Chl (including an outlier at day 9 BAC+), d) C:N, e) C:Chl, and f) N:Chl. Dotted lines show the model fit without additional Carbon excretion term x_f. At day 8 the threshold for silicate limitation is reached leading to reduced photosynthesis (by the factor given by Si_{PS}) and inhibited Chl synthesis, which is visible as sharp transitions in POC and Chl.

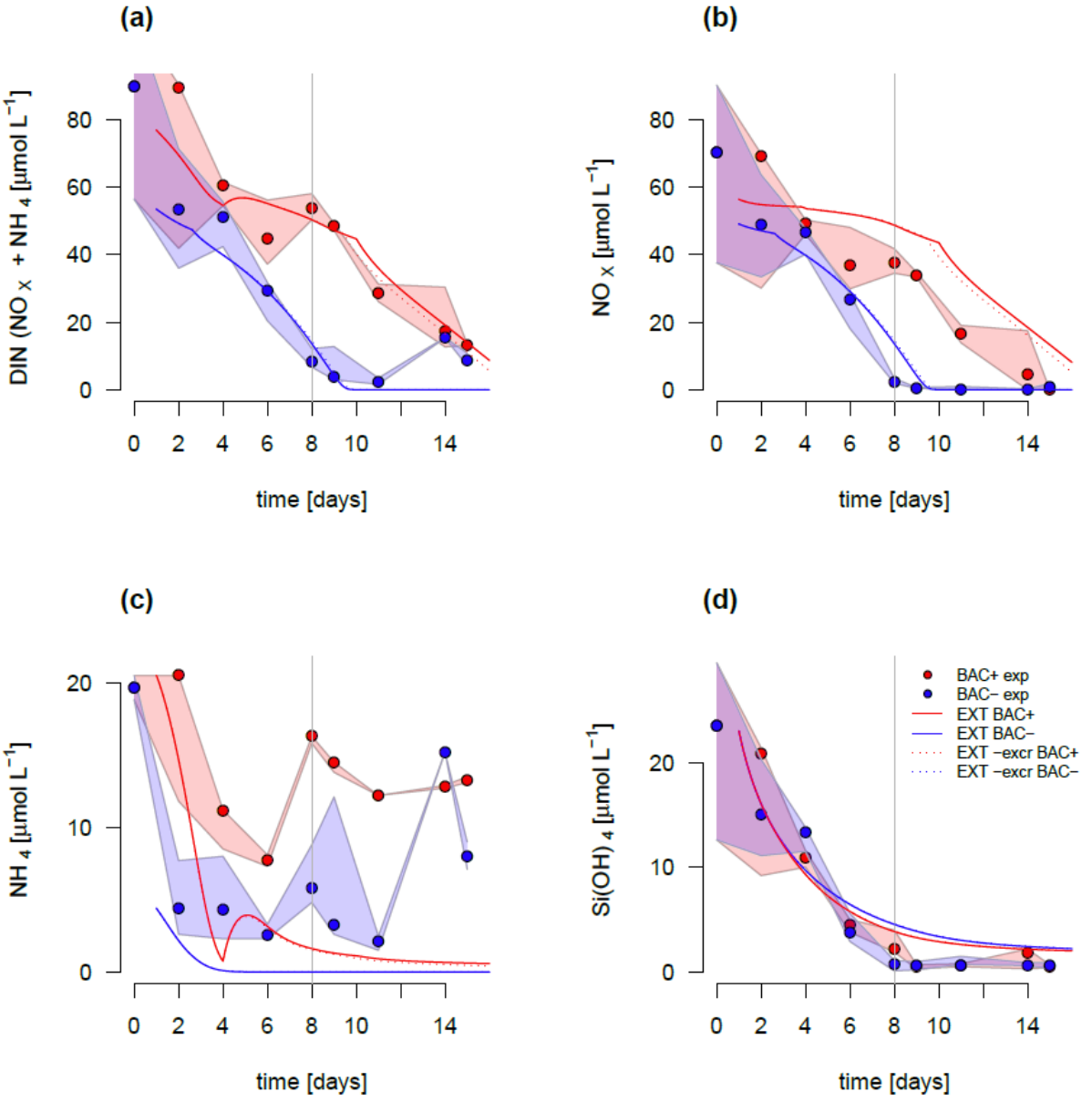

1025 Figure 6. Model fit of the EXT model to the BAC- (blue) and BAC+ (red) experiment. Circles show median values and the colored polygons show the maximum and minimum of measured data (n=3). Solid lines show the model outputs of a) DIN (NOX and NH4), b) NO_X, c) NH_4, and d) $Si(OH)_4$ (All model fits overlap).

Table

Table 1. A comparison of major components contributing to the complexity of different models discussed. #param is the number of parameters. In case of ecosystem models (SINMOD, BFM, MEDUSA, LANL, NEMURO, NPZD only the model formulations representing the components of the current model (phytoplankton growth, remineralisation, nutrient dynamics) are considered. For the full ecosystem scale models we give the original reference to the biogeochemical compartment of the ecosystem scale models and examples for more recent versions with updated formulations of other model compartments (e.g. physical drivers). REM designates those models that include Remineralisation (Rem) marked with V is present and X is absent. Ratios shows if the stoichiometry in the model considers variable or fixed ratios of intracellular elements (C:N:Si:P:Fe). The Nutrients considered are given under Nutrients. If DIN is considered as both NH_4 and NO_3, N is shown as N^2. MEDUSA has Fe dependent Si:N ratios, which makes them fixed in the Arctic (fixed*).

Model	Reference	#param	Rem	ratios	Nutrients
		Culture scale			
EXT	This study	21[*1]	V	variable	N^2, Si
G98	Geider et al., 1998	10[*2]	X	variable	N
ANIM	Flynn, 1997	30	V	variable	N^2
SHANIM	Flynn and Fasham, 1997	23	X	variable	N^2
Flynn01	Flynn, 2001	54	X	variable	N^2, Si, P, Fe
Flynn18	Flynn et al., 2018	27	X	variable	N
		Ecosystem scale			
BFM	Vichi et al., 2007	54	V	variable	N^2, Si, P, Fe
BFM17	Smith et al., 2020	24	V	variable	N^2, P
REcoM-2	Hauck et al., 2013 Schourup-Kristensen et al. 2018	28	X	variable	N, Si, Fe
MEDUSA	Yool and Popova, 2011 Henson et al., 2018	21	V	fixed*	N, Si, Fe
LANL	Moore et al., 2004	15	V	fixed	N^2, Si, P, Fe
NEMURO	Kishi et al., 2007 Amju et al., 2020	21	V	fixed	N^2, Si
NPZD	Gruber et al., 2006	9	V	fixed	N^2
SINMOD	Wassmann et al., 2006 Alver et al., 2016	12	X	fixed	N^2, Si

Degrees of freedom after constraints by the measured data are [*1]14 and [*2]6

Appendix

Tables

Table A1. State variables of the G98 model and the EXT model (marked with V if present and X if absent) with units and designation if these state variables had been measured in the experiment.

variable	Description	G98	EXT	Measured	Unit
DIN	Dissolved inorganic nitrogen	V	V	V	mgN m^{-3}
C	Particulate organic carbon	V	V	V	mgC m^{-3}
N	Particulate Nitrogen	V	V	V	mgN m^{-3}
Chl	Chlorophyll a	V	V	V	mgChl m^{-3}
Si_d	Dissolved Silicate	X	V	X	µmol L^{-1}
Si_p	Particulate/biogenic Silicon	X	V	V	mgSi m^{-3}
Bact	Bacteria cells	X	V	V	10^r. cells mL^{-1}
DONr	refractory dissolved organic nitrogen	X	V	V	mgN m^{-3}
DONl	labile dissolved organic nitrogen	X	V	X	mgN m^{-3}
NH4	Ammonium	X	V	V	µmol L^{-1}
NO3	Nitrate	X	V	V	µmol L^{-1}
Q	Particulate N : C ratio	X	V	X	gN gC^{-1}
θ^C	Chl to POC ratio	X	V	X	gChl gC^{-1}
θ^N	Chl : phytoplankton nitrogen ratio	X	V	X	gChl gN^{-1}

Table A2. Parameters of the original G98 model and the model extension with associated units.

parameter		Unit
	G98	
ζ	cost of biosynthesis	gC gN^{-1}
R^C	The carbon-based maintenance metabolic rate	d^{-1}
θ^N_{max}	Maximum value of Chl:N ratio	gChl gN^{-1}
Q_{min}	Min. N:C ratio	gN gC^{-1}
Q_{max}	Max. N:C ratio	gN gC^{-1}
α^{Chl}	Chl-specific initial C assimilation rate	gC m^2 (gChl µmol photons)$^{-1}$
I	Incident scalar irradiance	µmol photons s^{-1} m^{-2}
n	Shape factor for V^N_{max} max photosynthesis	-
K_{no3}	Half saturation constant for nitrate uptake	µmol L^{-1}
P^C_{ref}	Value of max C specific rate of photosynthesis'	d^{-1}
	Extension	
x_f	Carbon excretion fraction	-
K_{si}	Half saturation constant for Si uptake	µmol L^{-1}
V_{max}	maximum Si uptake rate	mol Si d^{-1} mg C^{-1}
s_{min}	minimum Si required for uptake	µmol L^{-1}
rem	remineralisation rate of excreted don	$bact^{-1}$ d^{-1}
rem_d	remineralisation rate of refractory don	$bact^{-1}$ d^{-1}
μ_{bact}	bacteria growth rate	mio. cells mL^{-1} d^{-1}
$bact_{max}$	Carrying capacity for bacteria	mio. cells mL^{-1}
K_{nh4}	Half saturation constant for ammonium uptake	µmol L^{-1}
$nh4_{thres}$	threshold concentration for ammonium uptake	µmol L^{-1}
Si_{PS}	Fraction of photosynthesis possible after Si lim.	-

Table A3. Parameters of the original G98 model and the EXT model with initial values used in the model and the lower and upper value constraints used for model fitting, unless the parameter was already defined by the data (measured). The constraints are either based on G98 fits to other diatom species, to present experimental data, or to typical values found in the literature.

parameter	value	lower	upper	constrained by
G98				
ζ	1	1	2	G98
R^C	0.01	0.01	0.05	G98
θ^N_{max}	1.7	measured		Data
Q_{min}	0.05	measured		Data
Q_{max}	0.3	measured		Data
α^{Chl}	0.076	0.075	1	G98
I	100	measured		Data
n	3.45	1	4	G98
K_{no3}	2	1	10	G98
P^C_{ref}	0.8	0.5	3.5	G98
Extension				
x_f	0.06	0.01	0.3	Schartau et al., 2017
K_{si}	7.6	0.5	8	Werner 1978
V_{max}	0.1	0.05	0.9	Data
s_{min}	1.82	1.5	6	Werner 1978
rem	10	10	20	open (rem > rem_d)
rem_d	4.55	0.1	10	open (rem_d < rem)
μ_{bact}	0.04	0.01	0.79	Data
$bact_{max}$	0.015	0.005	0.1	Data
K_{nh4}	6.7	0.5	9.3	Eppley 1969
$nh4_{thres}$	1.12	0.1	10	open
Si_{PS}	0.2	0	0.5	Werner 1978

Table A4. Output of the sensitivity analysis (senFun of the FME package in R) with the value for each parameter and different sensitivity indices obtained after quantifying the effects of small perturbations of the parameters.on the output variables (POC, PON, Chl, DIN). The L1 and L2 norms are normalized sensitivity indices defined as $L1 = \sum \frac{|S_{i,j}|}{n}$ and $L2 = \sqrt{\frac{S_{i,j}^2}{n}}$ with $S_{i,j}$ being the the sensitivity of parameter i for model output j.

par	value	L1	L2	Mean	Min	Max
			G98			
ζ	1.00	0.10	0.19	-0.02	-0.15	0.98
R^C	0.07	0.04	0.05	-0.03	-0.08	0.14
θ^N_{max}	1.70	0.23	0.34	0.14	-1.00	0.58
Q_{min}	0.05	0.06	0.08	-0.04	-0.14	0.22
Q_{max}	0.30	0.34	0.47	-0.24	-1.90	0.28
α^{Chl}	0.08	0.20	0.29	-0.10	-1.10	0.20
I	100	0.20	0.29	-0.10	-1.10	0.20
n	3.40	0.33	0.75	0.03	-0.47	4.07
K_{no3}	2.00	0.01	0.02	0.00	-0.01	0.09
P^C_{ref}	0.80	0.82	1.48	0.16	-7.70	1.04
			EXT			
x_f	0.06	0.19	0.27	-0.10	-0.37	1.10
K_{si}	7.6	0.00	0.00	0.00	0.00	0.00
V_{max}	0.1	0.00	0.00	0.00	0.00	0.00
s_{min}	1.82	0.00	0.00	0.00	0.00	0.00
rem	10	0.00	0.00	0.00	0.00	0.00
rem_d	4.55	0.24	0.31	0.24	0.00	0.65
μ_{bact}	0.04	0.00	0.00	0.00	0.00	0.01
$bact_{max}$	0.015	0.00	0.00	0.00	0.00	0.01
K_{nh4}	6.74	0.08	0.11	-0.03	-0.25	0.46
$nh4_{thres}$	1.19	0.00	0.00	0.00	0.00	0.00
Si_{PS}	0.2	0.08	0.24	-0.02	-1.40	0.31

Table A5. Other parameters calculated and used in the model equations

parameter	Description	Unit
P^{C}_{phot}	C-specific rate of photosynthesis	d^{-1}
P^{C}_{max}	Maximum value of P^{C}_{phot} at temperature T	d^{-1}
R^{Chl}	Chl degradation rate constant	d^{-1}
R^{N}	N remineralization rate constant	d^{-1}
V^{C}_{nit}	Diatom carbon specific nitrate uptake rate	gN $(gC\ d)^{-1}$
V^{C}_{ref}	Value of V^{C}_{max} at temperature T	gN $(gC\ d)^{-1}$
p_{Chl}	Chl synthesis regulation term	-
μ	specific growth rate of algae	cells d^{-1}

Table A6. Model equations from G98 (Geider et al., 1998) corrected for typographical errors by Ross and Geider (2009) with extensions.

1)	Carbon synthesis (C originates from unmodelled excess pool of DIC)	$\frac{dC}{dt} = \left(P^C - \zeta V_N^C - R^C\right)C = \mu C$
2)	Chl synthesis	$\frac{dChl}{dt} = \left(\frac{\rho_{Chl} V_N^C}{\Theta^C} - R^{Chl}\right) Chl$
3)	Nitrogen uptake	$\frac{dN}{dt} = \left(\frac{V_N^C}{Q} - R^N\right) N$
4)	from Eq. (1) and (2)	$\frac{dQ}{dt} = V_N^C - \mu Q$
5)	from Eq. (1) and (2)	$\frac{d\Theta^C}{dt} = V_N^C \rho_{Chl} - \Theta^C \mu$
6)	Photosynthesis	$P^C = P_{max}^C \left[1 - exp\left(-\frac{I}{I_K}\right)\right]$
7)	Max. N uptake	$V_N^C = V_{ref}^C \left[\frac{Q_{max} - Q}{Q_{max} - Q_{min}}\right] \frac{DIN}{DIN + K_{no3}}$
8)	with	$\rho^{Chl} = \Theta_{max}^N \left[1 - exp\left(-\frac{I}{I_K}\right)\right]$
9)		$V_{ref}^C = P_{ref}^C Q_{max}$
10)		$P_{max}^C = P_{ref}^C \frac{Q - Q_{min}}{Q_{max} - Q_{min}}$
11)		$I_K = \frac{P_{max}^C}{\alpha^{Chl} \Theta^C}$

1125

Table A7. Model equations of the EXT model based on G98

1a)	Carbon synthesis *(Reduced C synthesis under Si limitation after Werner 1978)*	$IF\ (Si_d < 2\ s_{min})$ $Si_{PS} = Si_{PS}$ $ELSE$ $Si_{PS} = 1$
1b)		$\frac{dC}{dt} = Si_{PS}\left(P^C - \zeta V_N^C - R^C - xf\right)C = \mu C$
2)	Chl synthesis *(Chl synthesis stops under Si limitation after Werner 1978)*	$IF\ (Si_d < 2\ s_{min})$ $\frac{dChl}{dt} = 0$ $ELSE$ $\frac{dChl}{dt} = \left(\frac{\rho_{Chl} V_N^C}{\Theta^C} - R_{Chl}\right) Chl$
3)	from Eq. (1 & 2)	$\frac{dQ}{dt} = V_N^C - \mu Q$
4)	from Eq. (1 & 2)	$\frac{d\Theta^C}{dt} = V_N^C \rho_{Chl} - \Theta^C \mu$
5)	Nitrogen uptake	$\frac{dN}{dt} = \left(\frac{V_N^C}{Q} - R^N - xf\right) N$
6)	Bacteria biomass production *(Logistic growth)*	$\frac{dBact}{dt} = Bact\ \mu_{Bact}\ (Bact_{max} - Bact)$
7a)	Silicate uptake *(Monod kinetics after Spilling et al., 2010)*	$\frac{dSi_d}{dt} = V_S^C = \left(V_{max} Si_d\ \frac{Si_d - S_{min}}{K_{si}\ S_{min}}\right) C$

7b)

$$\frac{dSi_p}{dt} = -\frac{dSi_d}{dt}\ 14$$

8) Ammonium uptake and production

(Threshhold after Tezuka 1989, and Gilpin 2004)

$$IF\ (\frac{C}{N} < 10)$$

$$\frac{dNH4}{dt} = \frac{-\left(\frac{V_{NH4}^C}{Q}\right)N + Bact\ xf\ N\ rem + Bact\ DON\ rem_d - \frac{Bact}{16})}{14\ 10^3}$$

$$ELSE$$

$$\frac{dNH4}{dt} = \frac{-\left(\frac{V_{NH4}^C}{Q}\right)N + Bact\ xf\ N\ rem - \frac{Bact}{16})}{14\ 10^3}$$

9) DON uptake and production

$$IF\ (\frac{C}{N} < 10)$$

$$\frac{dDON}{dt} = -\frac{Bact\ xf\ N\ rem + Bact\ DON\ rem_d + xf\ N}{14\ 10^3}$$

$$ELSE$$

$$\frac{dDON}{dt} = -\frac{Bact\ xf\ N\ rem + xf\ N}{14\ 10^3}$$

10) DIN uptake

$$IF\ (NH4 > nh4_{thresh})$$

$$\frac{dDIN}{dt} = \frac{-\left(\frac{V_{NO3}^C}{Q}\right)N - \frac{Bact}{16}}{14\ 10^3}$$

$$ELSE$$

$$\frac{dDIN}{dt} = \frac{-0.2\left(\frac{V_{NO3}^C}{Q}\right)N - \frac{Bact}{16}}{14\ 10^3}$$

11) Photosynthesis

$$P^C = P_{max}^C\left[1 - exp\left(-\frac{I}{I_K}\right)\right]$$

12a)	Max NO3 uptake	$V_{NO3}^{C} = V_{ref}^{C}\left[\frac{Q_{max} - Q}{Q_{max} - Q_{min}}\right]\frac{NO3}{NO3 + K_{no3}}$
12b)	Max NH4 uptake *(based on SHANIM Eq4 by Flynn and Fasham, 1997)*	$V_{NH4}^{C} = (0.01\,Q)\,0.0021\,\frac{NH4}{NH4 + K_{nh4}}$
13)	Max N uptake *(Based on Flynn and Fasham, 1997 and Flynn, 1999 showing no total inhibition in cold water)*	$IF\ (NH4 > nh4_{thresh})$ $V_{N}^{C} = V_{NH4}^{C} + 0.2\,V_{NO3}^{C}$ $ELSE$ $V_{N}^{C} = V_{NH4}^{C} + V_{NO3}^{C}$
14)	with	$\rho^{Chl} = \Theta_{max}^{N}\left[1 - exp\left(-\frac{I}{I_K}\right)\right]$
15)		$V_{ref}^{C} = P_{ref}^{C} Q_{max}$
16)		$P_{max}^{C} = P_{ref}^{C}\frac{Q - Q_{min}}{Q_{max} - Q_{min}}$
17)		$I_K = \frac{P_{max}^{C}}{\alpha^{Chl}\Theta^{C}}$

1130

Table A8. Output of the collinearity or parameter identifiability analysis using the collin function of the FME R package (Soetart et al., 2010b). A subset of any combinations of two parameter with a collinearity above 20, indicating non-identifiable parameter combinations is given (Brun et al., 2001).

ζ	R^C	θ^N_{max}	Q_{min}	Q_{max}	α^{Chl}	I	n	K_{no3}	P^C_{ref}	collinearity
1	0	1	0	0	0	0	0	0	0	31
1	0	0	0	1	0	0	0	0	0	59
1	0	0	0	0	1	0	0	0	0	42
1	0	0	0	0	0	1	0	0	0	42
1	0	0	0	0	0	0	1	0	0	74
0	1	0	0	0	0	0	0	0	1	22
0	0	1	0	1	0	0	0	0	0	32
0	0	1	0	0	1	0	0	0	0	26
0	0	1	0	0	0	1	0	0	0	26
0	0	1	0	0	0	0	1	0	0	41
0	0	0	0	1	1	0	0	0	0	49
0	0	0	0	1	0	1	0	0	0	49
0	0	0	0	1	0	0	1	0	0	81
0	0	0	0	0	1	1	0	0	0	1756319
0	0	0	0	0	1	0	1	0	0	60
0	0	0	0	0	0	1	1	0	0	60

Figure

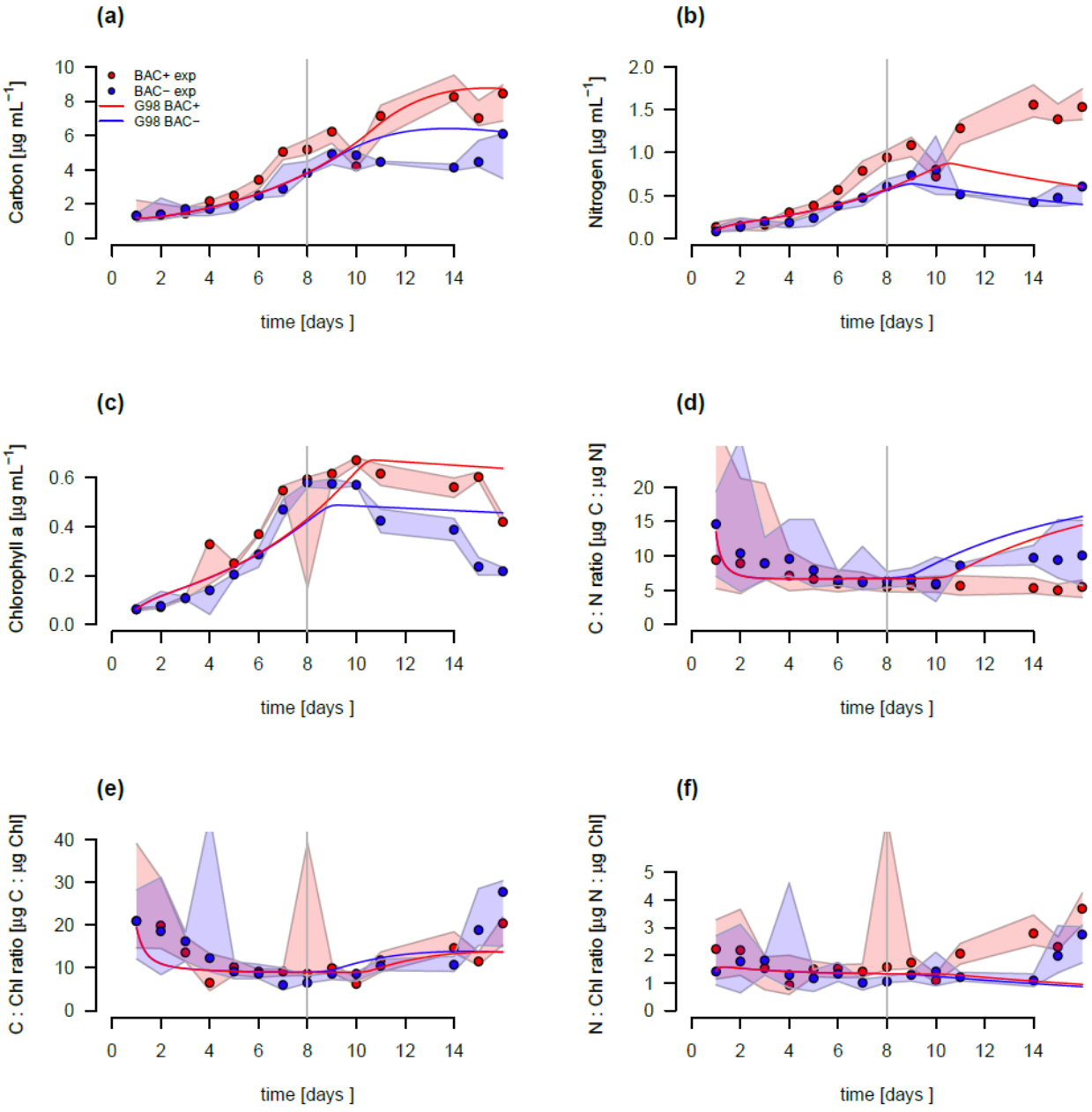

Figure B1: Model fit of the G98 model to the BAC- (blue) and BAC+ (red) experiment. Circles show median values and the colored polygons show the minimum and maximum of the measured data (n=3). Solid lines show the model outputs of a) POC, b) PON, c) Chl (including outlier at day 8 in BAC+), d) C:N, e) C:Chl, and f) N:Chl.

Equations

Equation C1. F-ratio estimation in the cultivation experiments with the average PON concentrations at day 13 to 15 ($PON^{d13\text{-}15}$) for the BAC- and BAC+ treatments.

$$f-ratio = \frac{PON_{BAC-}^{d13-15}}{PON_{BAC-}^{d13-15} + PON_{BAC+}^{d13-15}}$$

Equation C2. normalized RMSE with i being the different variables (POC, PON, Chl, DIN), and j the different values of each state variable. Predicted values are given as P and observed values as O.

$$RMSE = \sqrt{\sum_{\substack{i=1 \\ j=1}}^{n,p} \frac{(P_{i,j} - O_{i,j})^2}{Var(O_i)}}$$